LITHOFACIES, DEPOSITION, EARLY DIAGENESIS, AND POROSITY OF THE UTELAND BUTTE MEMBER, GREEN RIVER FORMATION, EASTERN UINTA BASIN, UTAH AND COLORADO

S. Katherine Logan, J. Frederick Sarg, and Michael D. Vanden Berg

OPEN-FILE REPORT 652
UTAH GEOLOGICAL SURVEY
a division of
UTAH DEPARTMENT OF NATURAL RESOURCES
in cooperation with the
U.S. GEOLOGICAL SURVEY
2016

LITHOFACIES, DEPOSITION, EARLY DIAGENESIS, AND POROSITY OF THE UTELAND BUTTE MEMBER, GREEN RIVER FORMATION, EASTERN UINTA BASIN, UTAH AND COLORADO

S. Katherine Logan[1], J. Frederick Sarg[1], and Michael D. Vanden Berg[2]

[1] Department of Geology & Geological Engineering,
Colorado School of Mines, Golden, CO; corresponding author, jsarg@mines.edu

[2] Utah Geological Survey, Salt Lake City, UT

Cover photo: *Transition from the fluvial Wasatch Formation (red slope) to the lacustrine carbonates and mudstones of the Uteland Butte member of the Green River Formation, eastern Uinta Basin.*

OPEN-FILE REPORT 652
UTAH GEOLOGICAL SURVEY
a division of
UTAH DEPARTMENT OF NATURAL RESOURCES
in cooperation with the
U.S. GEOLOGICAL SURVEY
2016

STATE OF UTAH
Gary R. Herbert, Governor

DEPARTMENT OF NATURAL RESOURCES
Michael Styler, Executive Director

UTAH GEOLOGICAL SURVEY
Richard G. Allis, Director

PUBLICATIONS
contact
Natural Resources Map & Bookstore
1594 W. North Temple
Salt Lake City, UT 84114
telephone: 801-537-3320
toll-free: 1-888-UTAH MAP
website: mapstore.utah.gov
email: geostore@utah.gov

UTAH GEOLOGICAL SURVEY
contact
1594 W. North Temple, Suite 3110
Salt Lake City, UT 84114
telephone: 801-537-3300
website: geology.utah.gov

CONTENTS

FIGURES

TABLES

LITHOFACIES, DEPOSITION, EARLY DIAGENESIS, AND POROSITY OF THE UTELAND BUTTE MEMBER, GREEN RIVER FORMATION, EASTERN UINTA BASIN, UTAH AND COLORADO

S. Katherine Logan, J. Frederick Sarg, and Michael D. Vanden Berg

ABSTRACT

The Uteland Butte member of the lower Green River Formation in the eastern part of Utah's Uinta Basin was correlated and mapped from outcrop to the subsurface using lithofacies and sequence-stratigraphic boundaries. The study area extends from the outcrop on the western side of the Douglas Creek Arch where lake-margin sediments occur, to cores from the Greater Natural Buttes natural gas field in central Uintah County, where sublittoral facies are predominant.

Eighteen facies and eight facies associations were described in the Uteland Butte section. Facies were identified based on lithology, grain size, texture, sedimentary structures, bed thickness, bed boundaries, and geometries and include: (F1) grey/green siltstone, (F2) lime to dolomitic mudstone, (F3) ostracod lime mudstone-wackestone, (F4) molluscan lime wackestone-packstone, (F5) oolitic lime mudstone-wackestone, (F6) intraclastic-ostracod lime packstone-grainstone, (F7) ostracod lime packstone-grainstone, (F8) oolitic lime packstone- grainstone, (F9) oncolite-ooid lime packstone-grainstone, (F10) ooid-pisolite lime packstone-grainstone, (F11) bioclastic lime floatstone to rudstone, (F12) ostracod-bearing sandstone, (F13) structureless to laminated sandstone, (F14) cross-stratified sandstone, (F15) carbonaceous shale, (F16) laminated illitic claystone, (F17) argillaceous mudstone, and (F18) laminated silty oil shale. Sedimentary facies are grouped into eight facies associations based on lateral and vertical relationships of depositional environments, energy level of the lake water, and relative water depth and include: (FA-A) fluvial-deltaic deposits, (FA-B) shoreline carbonate mudstone, (FA-C) littoral to sublittoral claystone to sandstone, (FA-D) carbonate shoal, (FA-E) microbial carbonate, (FA-F) littoral to sublittoral bioclastic mudstone to wackestone, (FA-G) littoral to sublittoral oil shale, and (FA-H) laminated oil shale.

On the eastern edge of the lake basin, where a ramp margin persisted and deltaic and fluvial influences were minor, outcrops show lake-margin environments that underwent four major flooding events. These cycles are correlated into the deeper regions of the lake using cores from the Greater Natural Buttes natural gas field area. Sublittoral successions from deeper in the lake are 30% thicker than the marginal Uteland Butte successions and are lean in silt and richer in dolomite—nearly every bed deposited in the sublittoral environment contains greater than 25% dolomite.

The Uteland Butte member contains rare stromatolites and lacks evaporites and analcime, but bivalves, gastropods, and ostracods are abundant across the study area, indicating a fresh water lake environment. Mud occurs in three forms: calcite, dolomite, and clay. Dolomite displays intercrystalline porosity averaging between 7 and 17%. Dolomitic mud found in packstones and grainstones occurs primarily as grain coatings, intraclasts, and peloids.

INTRODUCTION

The Uinta Basin, located in northeastern Utah and northwestern Colorado, is recognized for its organic-rich, Eocene-aged, lacustrine deposition (Bradley, 1931; Cole and Picard, 1978; Dyni and Hawkins, 1981; Hasiotis and Honey, 2000). Lacustrine systems are widely known to be sensitive to minor changes in accommodation and climate because of the smaller volumes of water and sediment compared to marine systems (Bohacs and others, 2000). Fluctuations in lake water levels can be rapid and are preserved in lake sediments that show distinctive vertical and lateral variations in stratigraphic units like the Green River Formation.

This study focuses on the lacustrine lithofacies, depositional processes, and diagenesis of the eastern portion of the Uteland Butte member of the lower Green River Formation; the formation's first major, widespread lacustrine unit. This interval is characterized by limestone, dolomite, organic-rich-calcareous mudstone, siltstone, and rare sandstone beds (Morgan and others, 2003). Dolomitized sections in the western portion of the basin act as hydrocarbon reservoirs which have porosity values commonly above 20% but low permeability due to very fine to microcrystalline fabric, and are targeted via horizontal drilling (Vanden Berg and others, 2014; Birdwell and others, in press).

The main goal of this study was to develop an integrated, subsurface to outcrop, sequence-stratigraphic framework for the depositional systems and lateral facies relationships of the carbonates and siliciclastics in the Uteland Butte on the eastern, non-productive, side of the Uinta Basin. In addition, this study includes a cursory characterization of the distribution and timing of dolomitization, including a description of pore types, dimensions, geometry, and distribution within the facies of the Uteland Butte member.

Previous Work

The Uteland Butte member represents the initiation of a lake environment at the end of deposition of the alluvial Wasatch Formation (Morgan and Bereskin, 2003). Bradley (1931) first described this unit on the western side of the Uinta Basin in Indian Canyon as the basal tongue of the Green River Formation. He considered this interval to be the first sediments of ancient Lake Uinta. The Uteland Butte member is equivalent to the basal limestone facies of Little (1988) and the Uteland Butte limestone of Osmond (1965). More recent work has been completed on the lower Green River Formation in the southwestern and western regions of the basin (Ryder and others, 1976; Remy, 1992; Wiggins and Harris, 1994; Keighley and others, 2003; Morgan and Bereskin, 2003; Taylor and Ritts, 2004; Burton and others, 2014), but little research has been completed on the eastern area where extensive outcrop exposures exist. Publications that focus on the eastern Uinta Basin are limited to general basin wide studies (Johnson, 1985a; Johnson, 1985b; Franczyk and others, 1992; Rosenberg and others, 2015). Johnson (1985a) completed a detailed study of the depositional history of the Piceance and Uinta Basins. The Green River tongue or Uteland Butte member in the eastern basin area is mentioned as a lime section rich in mollusks and ostracods (Johnson, 1985b). Most recently, the western portion of the Uteland Butte, which has been the target of significant hydrocarbon exploration, has been studied by Burton and others (2014), Vanden Berg and others (2014), and Birdwell and others (in press).

Tectonic Setting

The Uinta Basin is a structural and sedimentary basin formed in Late Cretaceous through early Tertiary time when rising Laramide uplifts broke up the Rocky Mountain foreland area into a number of smaller basins (Johnson, 1985a). These basins were separated by basement cored uplifts including the Uinta Mountains, Douglas Creek Arch, Uncompahgre Uplift, and the San Rafael Swell (figure 1). Laramide tectonism remained active throughout the Paleocene-Eocene depositional time interval of the Wasatch-Green River Formations (Franczyk and others, 1992). This tectonic activity, in combination with climatic changes, controlled lacustrine development in the early Eocene (Bohacs and others, 2000; Carroll and others, 2006; Davis and others, 2008, 2009).

The Uinta Basin is an asymmetrical foreland basin, with the largest sediment accumulations (greater than 4 km) close to the Uinta Uplift along the northern margin of the basin where subsidence was greatest (Fouch and others, 1992; Keighley and others, 2003). The more gently dipping southern margin of the basin experienced less subsidence and abundant sediment influx throughout the Paleocene and Eocene. The basins containing Green River sediments, including the Uinta Basin, are considered examples of ponded basins (Dickinson and others, 1988). During periods of high lake levels, the Uinta Basin on the west and the Piceance Basin on the east were connected into one large lake.

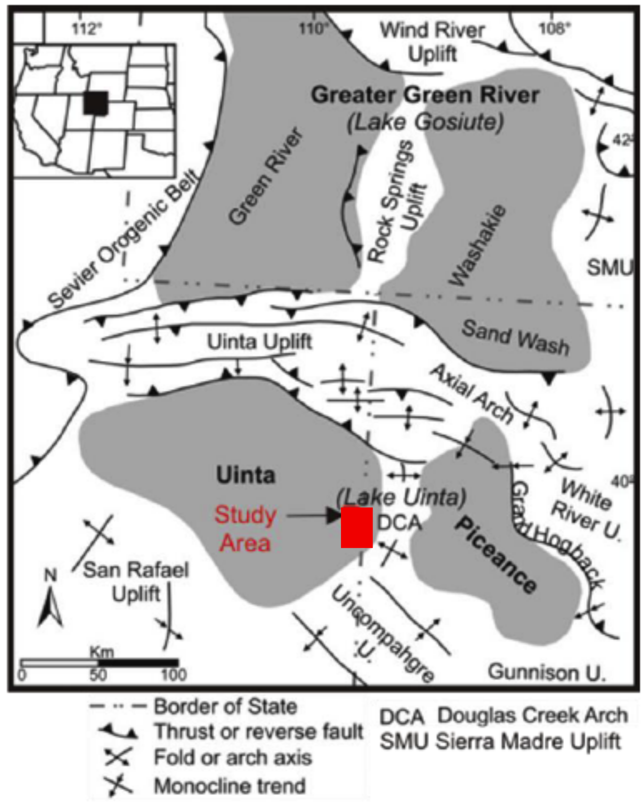

Figure 1. *Eocene intermountain lake basins and associated bounding uplifts in Colorado, Utah, and Wyoming (modified after Dickinson and others, 1988). Study area is outlined with red square.*

Field Area

The Uinta Basin is located in northeastern Utah and northwestern Colorado on the western edge of the Rocky Mountains. The basin lies almost entirely within the state of Utah and is separated from the related Piceance Basin by the Douglas Creek Arch (figure 1). The study area lies within Rio Blanco County, Colorado, and eastern Uintah County, Utah, in four main canyons: Hells Hole Canyon, Evacuation Creek, Texas Creek, and Missouri Creek, an area covering about 150 km^2 (figure 2). The outcrop locations are approximately 105 km southeast of Vernal, Utah, and run north-south along the Utah-Colorado state border.

Two Uteland Butte cores were made available to this project courtesy of Anadarko Petroleum Corporation. The addition of these cores from the Greater Natural Buttes natural gas field, approximately 60 km northwest of the outcrop areas, allowed for a depositional and stratigraphic transect from the eastern margin toward the basin center (figure 2). The drilling of the NBU 921-22M-GR well included recovery of 28 m of core, from 4826 to 4919 feet drill depth, with a 3.6 foot upward shift to match the geophysical logs, and covers nearly the entire Uteland Butte section. The NBU 921-18C4BS core consists of four recovered intervals in the lower Green River Formation. The lowest core, core 4, captures the upper 14.6 meters of the Uteland Butte, from about 5080 to 5128 feet drill depth, with a 1.5 foot downward shift to match the geophysical logs.

Stratigraphy

Deposition of the Green River Formation lacustrine sediments in Lake Uinta occurred over a roughly 10 million year period between about 54 to 44 Ma (Picard, 1957; Ryder and others, 1976; Smith and others, 2008, 2010; Davis and others, 2010). The Green River Formation lies above and is interbedded with the uppermost variegated shale, sandstone, and conglomerate fluvial deposits of the Wasatch Formation in the east and the Colton Formation in the west (figure 3). Overall thickness of the Green River Formation varies across the Uinta Basin. The thickest sediment accumulations (>2000 m) are to the west-northwest, the location of the early paleo-depocenter and the longest lived portion of the lake. In contrast, the eastern-southeastern edge, closer to the outcrop, has an average lacustrine sediment thickness of 900 m (Ryder and others, 1976; Schamel, 2015).

The lower Green River Formation, in the southern basin area, is subdivided into two main stratigraphic intervals bounded by regionally correlative carbonate units. The oldest interval is the Uteland Butte member, a bioclast-bearing unit that represents the first widespread lake system in the Unita Basin. In

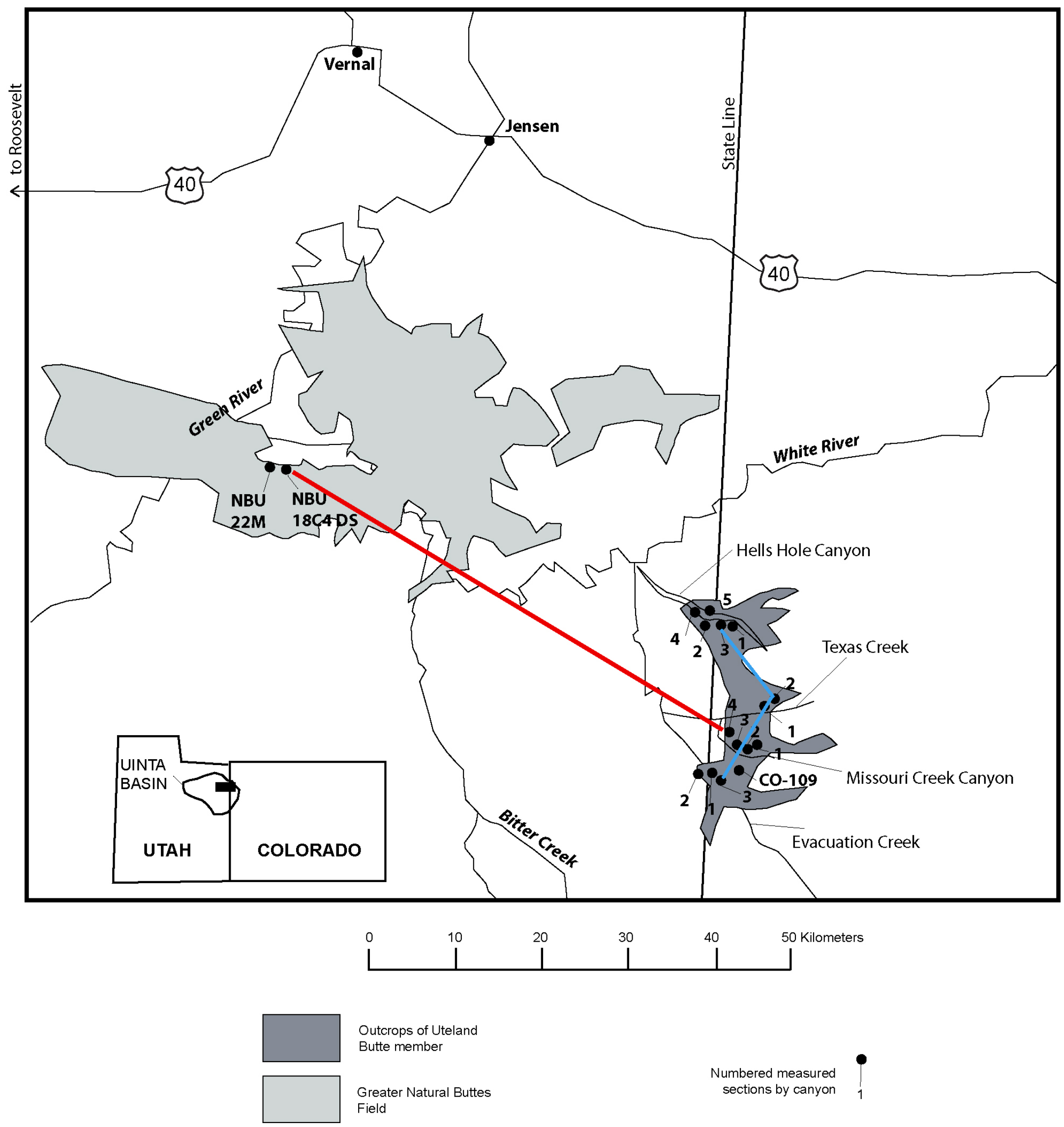

__Figure 2.__ Location map for eastern Uinta Basin study area, from eastern lake margin where outcrops lie along the Colorado-Utah border to cores from the Greater Natural Buttes natural gas field. A cross section along strike follows the blue line; a dip cross section from Missouri Creek to the Natural Buttes cores follows the red line.

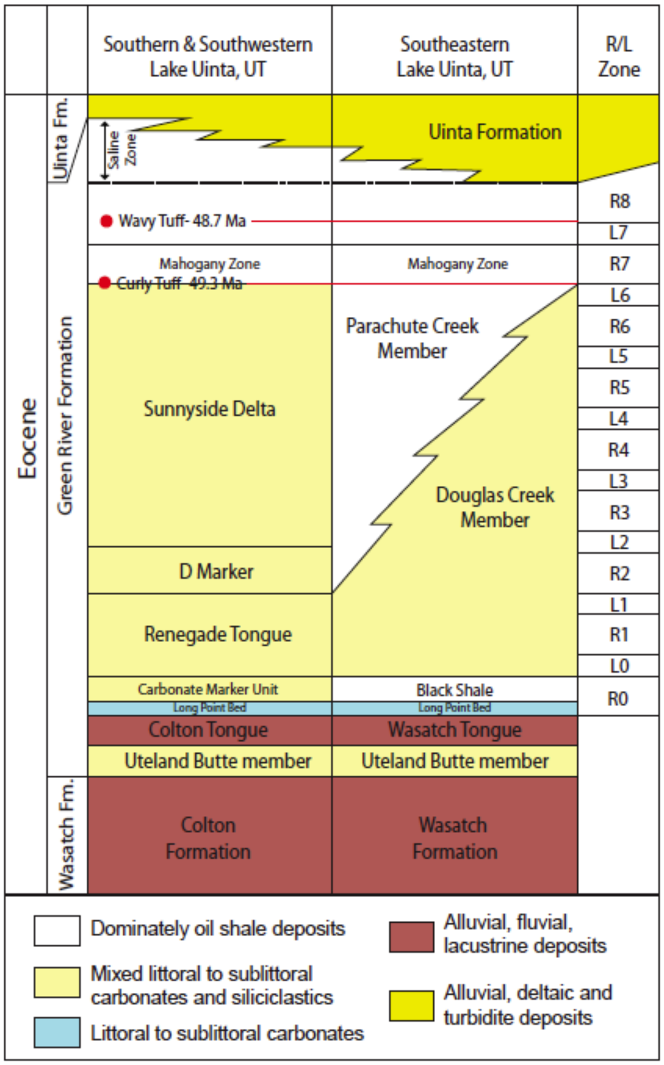

Figure 3. *Lithostratigraphic subdivision of the lower and middle Eocene deposits and correlation with kerogen-rich (R) and kerogen-poor (L) zones in the Uinta Basin (figure modified after Pitman, 1996; Dyni, 2006; Johnson and others, 2010; Self and others, 2010a, b; Tänavsuu-Milkeviciene and Sarg, 2012; Vanden Berg, 2008; rich and lean zones after Cashion and Donnell, 1972, 1974; Long Point Bed after Johnson, 1984). Rich and lean zones apply only for the deep lake deposits and cannot be used for correlation in the shallow marginal areas. Wavy and Curly Tuff numbers represent million years ago (Smith and others, 2010).*

the southern basin margin area, the Uteland Butte interfingers above and below with the alluvial-fluvial-lacustrine Wasatch Formation (figure 3). The upper Wasatch tongue in the east and the Colton tongue in the west are overlain by the second carbonate interval, the Carbonate Marker Unit which contains the Long Point Bed (Johnson, 1985a; Johnson, 1985b; Schomacker and others, 2010). The Long Point Bed overlies the Wasatch tongue in the study area and forms a distinctive bioclastic coquina interval that marks the beginning of the next transgression. The Black Shale Facies, which overlies the Long Point Bed, is equivalent to the upper portion of the Carbonate Marker Unit found farther to the west. Overlying the Black Shale Facies is the Douglas Creek Member of the Green River Formation, which is characterized by interbedded fluvial-deltaic and carbonate deposits (Abbott, 1957; Ryder and others, 1976). The Parachute Creek Member of the upper Green River Formation intertongues with these more proximal units and consists of finely laminated calcite and dolomite-rich mudstones deposited in alternating organic-rich (R) and lean (L) zones. These zones are interbedded with sparse siltstone and sandstone beds (Cashion and Donnell, 1972, 1974). The most consistent marker bed in the Green River Formation is the Mahogany oil-shale bed (within the R7), which lies within the Parachute Creek Member and represents Lake Uinta's highest water level (Johnson and others, 2010).

Uteland Butte Member

In the study area, the Uteland Butte member unconformably overlies a thick, variegated paleosol interval in the upper Wasatch Formation and is overlain by an alluvial pulse that comprises the uppermost Wasatch Formation or Wasatch tongue (Bradley, 1931; Ryder and others, 1976; Remy, 1992). The Uteland Butte member ranges in thickness from 15 to 65 m and consists of limestone, dolomite, organic-rich calcareous mudstone, siltstone, coquina, and occasional sandstone (figure 4). Along the eastern lake-margin, the Uteland Butte deposits are up to 22 m thick and consist of intermixed carbonate grainstone and mudstone beds. Ostracod and oolite-bearing grainstone beds, as thick as 2.5 m, are commonly interbedded with mixed mudstone and siltstone. The Uteland Butte member is a highly cyclic interval with centimeter to decimeter scale changes in outcrop and core (figure 4). The interval shows an overall coarsening upwards through time, and carbonate grainstone replaces the light green claystone and siltstone that dominate early lake deposits. The presence of ostracod and mollusks in the Uteland Butte member indicate that this unit was deposited in relatively clear and fresh lake waters that had little clastic input (Picard, 1957).

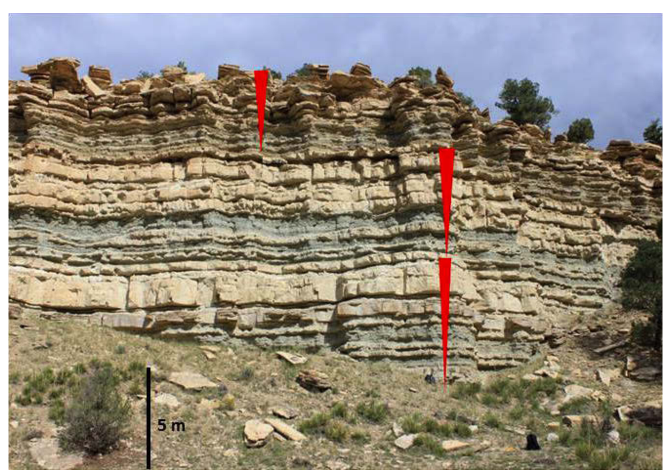

Figure 4. *White Face Butte outcrop at the Evacuation Creek 1 measured section (see figure 2) showing grey/green siltstone interbedded with light tan, bioclastic, lime packstones and grainstones. Red triangles indicate three shallowing up intervals in the Uteland Butte member.*

Depositional Cyclicity

A cycle is used to describe repetitive sedimentary successions interpreted to represent lacustrine expansion and contraction (Pietras and others, 2003). Several cycles are present within the Uteland Butte member (figure 4). Cycles in the lake margin region show shallowing upward sequence; a similar trend has been observed in other units of the Green River Formation on the southern and western side of the Uinta Basin (Eugster and Hardie, 1978; Smoot, 1983; Little, 1988). The cycles in the Uteland Butte range from 4 to 7 m thick on the margin and between 7 and 13 m in the deeper basin. These cycles are bounded by flooding surfaces in the form of littoral, lean oil shale and laminated ostracod siltstones along the eastern edge, and by black, laminated oil shale in the basin center. Flooding surfaces are commonly marked by intraclastic rudstone above, usually a few centimeters thick.

METHODOLOGY

This study integrated outcrop with subsurface data to construct a sub-regional correlation of the Uteland Butte member in northwestern Colorado and northeastern Utah. Fifteen outcrop sections were measured over 150 km^2 between Evacuation Creek and Hells Hole Canyon along the Colorado-Utah border. Sections range from 15 to 22 m in thickness and were measured on a centimeter scale to define lake level fluctuations and associated sedimentary cyclicity. The Uteland Butte is exposed in five canyons in this area including Evacuation Creek, Missouri Creek, Texas Creek, and Hells Hole Canyon (figure 2). In Hells Hole, the outcrops are continuous for about 8 km until they dip into the subsurface. Along strike variations can be assessed with a cross section transect from White Face Butte in the south to Missouri Creek, then Texas Creek, and finally to Hells Hole Canyon in the north. Sections in each respective canyon are anywhere from a 0.5 to 2 km apart, and distances between canyons vary between 3 and 24 km. Detailed descriptions identified lithology, nature of contacts, presence of fossils, organic-richness, and bed architecture.

Lithofacies and facies associations were defined for the outcrop sections and the two cores. Facies are primarily based on grain-size, depositional texture, fossil or bioclast abundance, and sedimentary structures. Facies associations were defined to represent distinctive depositional settings and are based on Gierlowski-Kordesch (2010).

Petrographic description was completed on thin sections from 41 outcrop samples within the Uteland Butte member and the Wasatch Formation. Thin sections, prepared for Anadarko by Weatherford Laboratories, from the core were also described. Descriptions include observations of porosity character, carbonate grain identification (calcite vs. dolomite), estimation of mineral percentages, and examination of rock microstructures.

Dip and strike cross sections were constructed from the outcrop into the subsurface (figure 2, red line is a depositional dip cross section and blue line represents a depositional strike cross section). This project focused only on an eastern to central basin correlation. In addition, these cross sections integrate data into a sub-regional depositional model and provide regional context on the nature of the facies changes and dolomite relationship in the basin. Correlative surfaces helped identify major cycles and were mapped using flooding surfaces.

Characterization of microporosity was undertaken using the QEMSCAN (***Q****uantitative* ***E****valuation of* ***M****inerals by* ***SCAN****ing* electron microscopy) analysis tool. QEMSCAN is an integrated system that consists of a Scanning Electron Microscope (SEM), four nitrogen-free Energy-Dispersive X-ray spectroscopy (EDS) detectors, and proprietary software to capture a wide spectrum of elemental abundance data on a pixel basis and to image pore size and architecture. Twelve samples, representing a distribution of lithofacies identified in outcrop and core were analyzed at the Colorado School of Mines for quantitative mineralogy, porosity, and grain size. These analyses provided information about dolomite distribution, clay mineralogy, porosity distribution, and pore geometry.

LITHOFACIES

Eighteen sedimentary facies are recognized in the Uteland Butte member within the study area. Facies were identified based on lithology, grain size, and sedimentary structures (table 1). Additional criteria for lithofacies identification include bed thickness, bed boundaries, and geometries. These facies are grouped into eight facies associations based on lateral and vertical relationships between the facies (table 2). Rock texture is based upon Dunham's classification (1962), with the Embry and Klovan (1971) modification (e.g., rudstone, floatstone). Classification of mixed siliciclastic-carbonate rocks containing between 10 to 50% terrigenous admixtures were distinguished in nomenclature from pure carbonates. Grains were not incorporated into the rock name until they compose >20% (for intraclasts, oncoids, or ooids) or >40% (for fossils and peloids) of the rock (Strohmenger and Wirsing, 1991).

Lacustrine zones in Lake Uinta have been defined by energy levels as: (1) the littoral zone above fair-weather wave base; (2) the sublittoral zone between fair weather wave base and storm wave base; and (3) the profundal zone below storm wave base (after Reading and Collinson, 1996; Cohen, 2003; Renaut and Gierlowski-Kordesch, 2010). The relative water depth is defined after Renaut and Gierlowski-Kordesch (2010) and Tänavsuu-Milkeviciene and Sarg (2012), where a shallow lake is described as a lake with only littoral and sublittoral zones and a deep lake is described as a lake with littoral, sublittoral, and profundal zones.

Table 1. *Lithofacies in the Uteland Butte member of the Green River Formation.*

	Lithofacies	Texture/lithology/ grain types	Structure	Thickness	Geometries and Contacts	Location	FA
1	Grey/Green Siltstone	Siliciclastic clay to silt	Laminated to massive	Laminated to very thick bed	Laterally continuous, sharp basal non-erosive contact	Littoral to sublittoral	A, C
2	Lime to Dolomitic Mudstone	Lime mud	Structureless, commonly graded or laminated	Medium to very thick bed	Laterally continuous, sharp contact	Littoral	A, B, F
3	Ostracod Lime Mudstone-Wackestone	Lime mud, ostracods, siliciclastic quartz particles, microbial	Ostracods, massive, graded, plane-parallel, cross-stratified	Very thin to thick	Laterally continuous, Sharp basal non-erosive contact	Littoral to sublittoral	B, C, E, F, G
4	Molluscan Lime Wackestone-Packstone	Lime mud, shells, siliciclastic clay particles	Bivalves, gastropods, structureless, wavy, plane-parallel	Laminated to thick	Sharp basal non-erosive contact, undulatory, gradational	Littoral to sublittoral	B, C, F, G
5	Oolitic Lime Mudstone- Wackestone	Lime mud, oolites, pisolites	Massive, plane-parallel	Thin bed	Sharp basal non-erosive contact	Littoral	B, C, F, G
6	Intraclastic-Ostracod Lime Packstone-Grainstone	Carbonate mud clasts, ostracods	Ostracod, mud clasts, structureless, ripple cross-laminations	Very thin to medium bed	Thin and undulatory, gradational	Littoral to sublittoral	C, D
7	Ostracod Lime Packstone-Grainstone	Ostracods, peloids, lime mud	Massive, plane-parallel, ripple cross-laminations	Very thin to very thick bed	Laterally continuous, sharp base, gradational, gravity flows	Littoral to sublittoral	C, D, F
8	Ooid Lime Packstone-Grainstone	Oolites, peloids, lime mud	Oolites, peloids, massive, plane-parallel	Very thin to very thick bed	Laterally continuous, sharp base	Littoral	D, E
9	Oncolite-Ooid Lime Packstone-Grainstone	Oncoids, lime mud, ostracod grains	Oncolites, lime mud, ostracod grains, quartz, massive	Thin	Gradational	Littoral	C, D, E
10	Ooid-Pisolite Lime Packstone-Grainstone	Pisoids, ostracods, lime mud	Pisolites, peloids, massive or plane-parallel	Thin to medium bed	Thin and discontinuous, gradational	Littoral	D
11	Bioclastic Lime Floatstone to Rudstone	Ostracods and shells, lime mud	Bivalves and gastropods >2mm, structureless or wavy	Very thin to thin bed	Sharp to gradational, laterally continuous	Littoral to sublittoral	D
12	Ostracod-Bearing Sandstone	Fine to medium sand, ostracods, shells, calcite	Ripple cross-laminations, massive	Medium to thick bed	Laterally continuous, sharp base, discontinuous	Littoral	C
13	Structureless to Laminated Sandstone	Fine to coarse grained sand	Structureless, graded, calcite	Thin to thick	Thick and discontinuous, sharp base	Littoral to sublittoral	A, C
14	Cross-Stratified Sandstone	Medium to coarse grained	Planar cross-stratified, high angle	Thick	Sharp lower contact	Shoreline	A
15	Carbonaceous Shale	Lignite	Finely laminated fine sediment, plant and organic material	Thin bed	Thin and continuous	Marshes and swamps	B
16	Laminated Illitic Claystone	Kerogen-rich mud, clay-rich	Parallel-laminated, occasionally ostracod rich, some silt to sand layers and lenses	Laminated to medium bed	Transitional, continuous	Littoral to sublittoral	F, G, H
17	Argillaceous Mudstone	Dolomitic mudstone with siliciclastic clay	Wavy, plane-parallel laminated	Thin to thick bed	Transitional to sharp base	Sublittoral	B, C, F, G, H
18	Laminated Silty Oil Shale	Dominantly dolomitic, kerogen-rich, with silt to very fine sand	Parallel-laminated, silt to sand layers and lenses	Laminated to medium bed	Transitional	Sublittoral to Profundal	G, H

Table 2. *Facies associations of the Uteland Butte member of the Green River Formation.*

FA	Facies Association	Description	Lithofacies
A	Fluvial-Deltaic Deposits	Sandstone channel and tabular bodies laterally and vertically associated with littoral to sublittoral siltstone and sandstone (FA-C), and laterally associated with shoreline mudstone (FA-B) and carbonate shoals (FA-D).	F1, F2, F12, F13, F14, F17
B	Shoreline Carbonate Mudstone	Calcareous and dolomitic mudstones are vertically associated with carbonate shoals (FA-D) and littoral to sublittoral siltstone (FA-C). In association with delta deposits (FA-A).	F2, F3, F4, F5, F15
C	Littoral to Sublittoral Claystone to Sandstone	Large, massive siltstones located down-dip from delta systems (FA-A), sandstones, thin and discontinuous.	F1, F2, F3, F4, F5, F6, F7, F8, F12, F13, F17
D	Carbonate Shoal	Laterally extensive marginal grainstone beds largely ostracod, intraclast and bivalve rich. Vertically and laterally associated with littoral to sublittoral siltstones (FA-C), and laterally associated with FA-A and FA-B.	F6, F7, F8, F9, F10, F11
E	Microbial Carbonate	Thin, wavy laminated, dominantly found mixed with dolomitic mud and ostracod shell beds in sublittoral environments. Vertically associated with littoral to sublittoral oil shale (FA-G), sublittoral siltstones and littoral to sublittoral bioclastic wackestone to mudstone (FA-F).	F3, F8, F9
F	Littoral to Sublittoral Bioclastic Mudstone to Wackestone	Distal carbonate and dolomite deposits with varying amounts of ostracod and bivalve grains. Laminated and laterally continuous. Laterally associated with littoral to sublittoral oil shale (FA-G), laminated oil shale (FA-H) and carbonate shoals, generally ostracod accumulations (FA-D).	F2, F3, F4, F7, F16, F17
G	Littoral to Sublittoral Oil Shale	Laminated silt-rich and kerogen poor oil shale. Laterally continuous. Laterally and vertically associated with carbonate shoals (FA-D), microbial deposits (FA-E) and littoral to sublittoral siltstones and sandstones (FA-C), and FA-F mudstones and wackestones.	F3, F4, F16, F17, F18
H	Laminated Oil Shale	Laterally extensive laminated oil shale with higher kerogen content and low silt percentages. Most distal deposit. Associated with FA-F.	F16, F17, F18

Lithofacies F1: Grey/Green Siltstone

Lithofacies F1 consists of greyish green, fissile mud to silt with varying organic material and includes ostracod and bivalve shells. Beds range from massive to thin and thick plane-laminated and range in thickness from 1 cm to thicker than 3 m. Calcareous content and concretions are found locally and compose up to 20% of this facies. Siliciclastic grains are angular to subrounded and range in size from fine silt to fine sand (figure 5A). Horizontal and vertical burrows are present and can be abundant.

Lithofacies F1 represents a unit mainly deposited from suspension fall-out in a quiet environment away from the higher energy shoreline, in the deeper littoral and sublittoral region. These beds contain abundant ostracods. Abundance of ichnofossils suggests a well-oxygenated lake bottom area. F1 is laterally adjacent to bioclastic rudstone beds, carbonate shoals, and sublittoral to littoral distal sandstone deposits. This facies is persistent throughout the outcrop area.

Lithofacies F2: Lime to Dolomitic Mudstone

Lithofacies F2 is dominantly microcrystalline calcite or dolomite, with between 10 to 30% clay to fine quartz silt, minor amounts of calcite spar, ostracods, pelecypod shells, and accessory minerals (figure 5B). F2 is structureless with some grading into coarser grained rock types. Microcrystalline calcite accounts for 90 to 95% of this facies. Undifferentiated bioclast grains are randomly oriented and angular to subangular in shape. Identifiable ostracod valves and bivalve shells account for less than 3% of matrix and are commonly broken and isolated. There are trace amounts of organic material and fish scales. Bed thickness ranges from 5 mm to >1m. Porosity in this facies is dominantly microporosity and is 1% or less.

Lithofacies F2 is interpreted to have been deposited by precipitation from the water column in calm shoreline environments and on carbonate mud flats. The fine-grained nature of this facies suggests a low-energy depositional environment and the bioclasts suggest oxic conditions with increased water circulation. The low influx of quartz grains suggests relatively great distances from deltaic and fresh water surface inputs into the lake.

Lithofacies F3: Ostracod Lime Mudstone-Wackestone

Lithofacies F3 is dominantly a microcrystalline lime mud with ostracod shells, minor amounts of siliciclastic quartz, and organic material (figure 5C). Beds generally exhibit massive, plane-parallel or cross-stratified laminations in coarser intervals. Ostracod shells are broken and whole and show random orientation, while quartz grains are randomly dispersed, subrounded to rounded, and silt to very fine sand in size. Beds are non-erosive and have a sharp base, and the bed thickness ranges from very thin to thick (1–100 cm).

This facies represents an environment with varying energy activity. The microcrystalline calcite material likely precipitated from the water column in calm water conditions. Ostracods are planktonic and fall out of suspension after death. Deposits in deeper water environments show fining upward

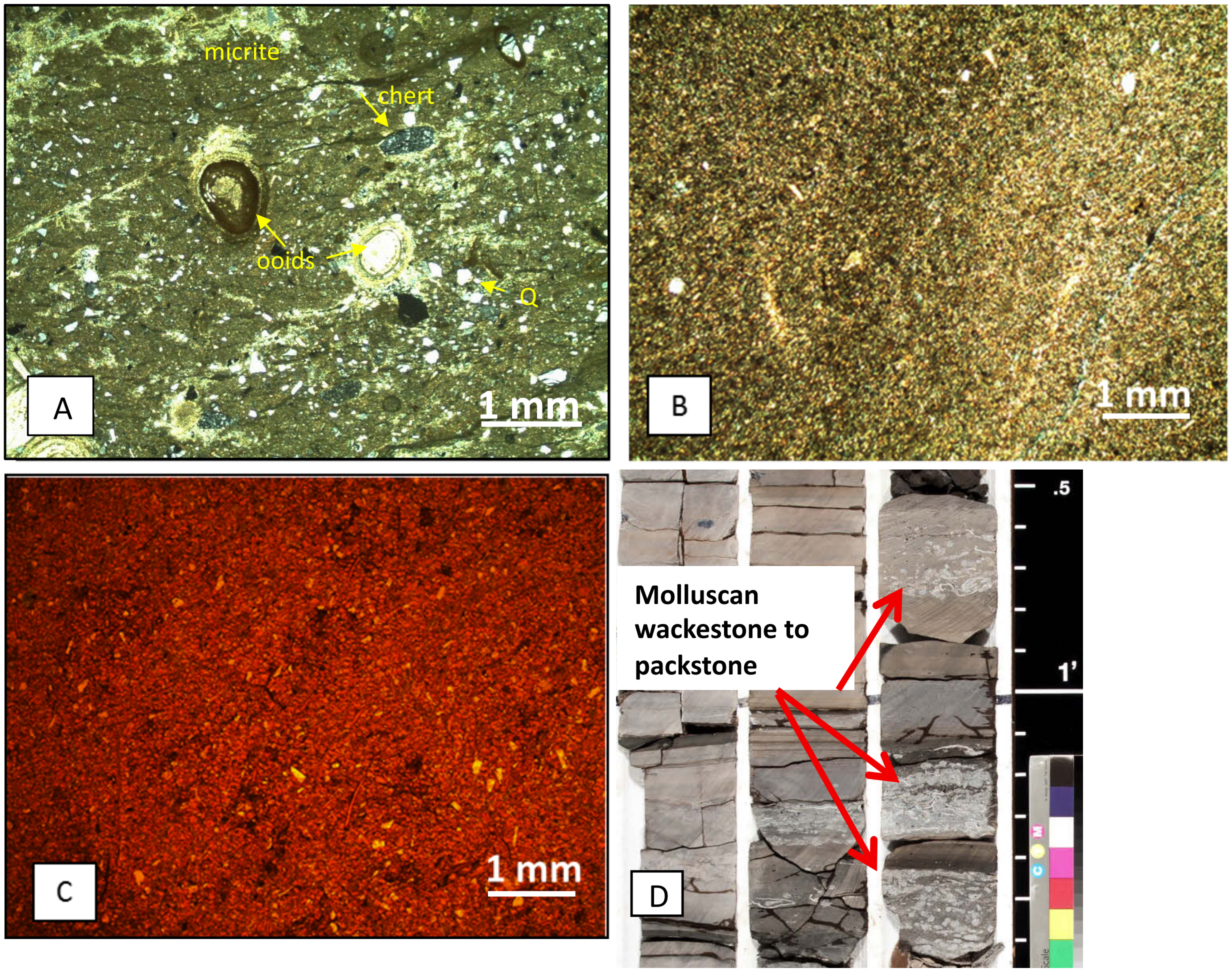

Figure 5. A. *F1 grey/green siltstone with superficial ooid grains, angular quartz (Q), chert, and micrite (Evacuation Creek 2);* ***B.*** *F2 lime to dolomitic mudstone (Evacuation Creek 2);* ***C.*** *F3 ostracod lime mudstone-wackestone (red alizarin stain) with black organic material and yellow quartz grains (Evacuation Creek 2);* ***D.*** *F4 molluscan lime wackestone-packstone from Anadarko NBU 921-22M core, depth range 4870 to 4872.2 feet.*

patterns in places and may have been brought into the distal littoral to sublittoral environment by turbidity flows, which can occur over mudflat (F2) areas extending out to deeper waters in the littoral to sublittoral regions where calm water persists. F3 beds are laterally adjacent to carbonate shoal deposits (F6, F7, F8, and F9), delta deposits (F12, 13, 14, and 17), and carbonate mudflats (F2).

Lithofacies F4: Molluscan Lime Wackestone-Packstone

Lithofacies F4 has a mineralogically homogeneous microcrystalline calcite matrix with bivalve, gastropod, and ostracod grains, and trace amounts of quartz and organic material (figure 5D). Beds are structureless to wavy, plane-parallel laminated, and the pelecypod shells are usually broken and oriented parallel to bedding. Siliciclastic material occurs as angular to subangular silt-sized grains. Beds are very thin to medium (1–30 cm) and have sharp, undulatory, non-erosive basal contacts.

F4 represents an environment with varying energy activity. Again, the microcrystalline calcite material is likely precipitated from the water column in calm water conditions. The biogenic shells suggest an oxic environment. This facies is interpreted to occur in two main areas, along the shoreline in a mudflat area where mollusks flourished or in distal littoral to sublittoral regions where calm water persists. F4 is laterally adjacent to carbonate shoals (F6, F7, F8, and F9) and carbonate mudflats (F2) and is observed in outcrop and core. This facies is dolomite-rich in the two basin center cores.

Lithofacies F5: Oolitic Lime Mudstone-Wackestone

Lithofacies F5 consists of calcareous and dolomitic microcrystalline mud with 5 to 15% sub-spherical ooids and trace amounts of ostracod remains and organic material (lens in figure 6A). F5 shows massive or plane-parallel laminations that are interlaminated with organic material. Bed thickness varies from 2 to 35 cm and displays sharp basal contacts.

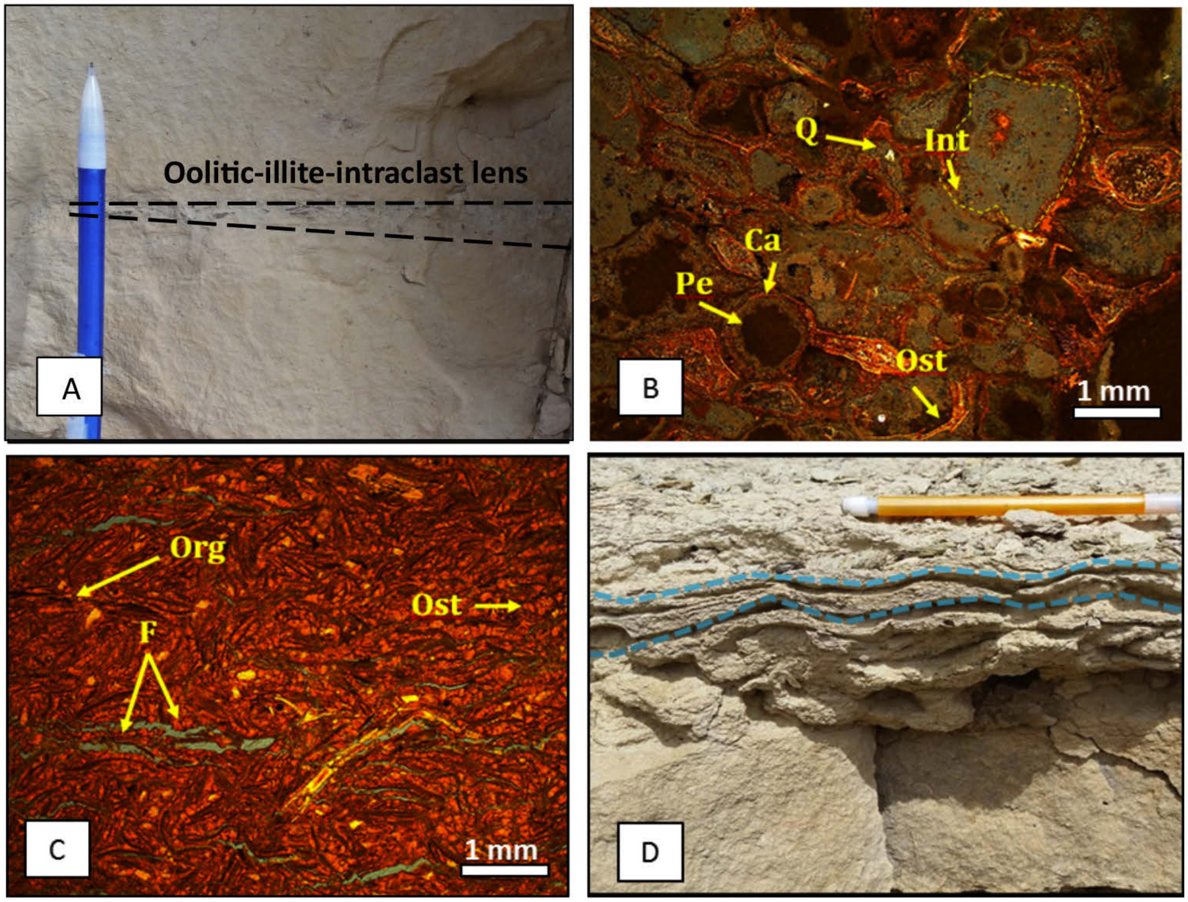

Figure 6. A. *F5 oolitic lime mudstone-wackestone with illite-intraclast lens in lime to dolomite mudstone (F2) (Hells Hole 3);* ***B.*** *F6 Intraclast-ostracod lime packstone-grainstone with intraclasts (Int), ostracods (Ost), quartz (Q), peloids (Pe), and lithified carbonate coating (Ca) (Texas Creek 1);* ***C.*** *F7 ostracod lime packstone-grainstone laminated with fractures (F), organic material (Org), and ostracods (Ost) (Evacuation Creek 3);* ***D.*** *F8 oolitic lime packstone-grainstone with wave-ripple laminations at the top of the bed (Texas Creek 2).*

This facies represents a moderate energy environment. Similar to lithofacies F2, F3, and F4, the calcareous mud is likely deposited as a precipitate from the supersaturated water column in a lower energy environment. Ooids require more energy to form and were probably carried into the system during storms or higher energy events from nearby grainstone deposits (F6, F7, F8, and F9) and are intermixed with F2 mudstone.

Lithofacies F6: Intraclastic Ostracod Lime Packstone-Grainstone

Lithofacies F6 is predominantly composed of intraclast and ostracod grains, with minor amounts of siliciclastic quartz, peloids, and ooids (figure 6B). The intraclasts are poorly sorted, closely packed, angular to subrounded, and range in size from medium sand to gravel (>2 mm) and are dominantly composed of microcrystalline dolomite (figure 6B). The associated ostracods shells are typically filled with dolomicrite and are whole or broken. These clasts are usually deposited with oncoids and broken ostracod pieces. Intraclasts and ostracods have high intraparticle and moldic porosity, with low associated permeability. Siliciclastic grains are rare in F6 and are silt (0.05 mm) in size. Calcite spar occurs as cement between intraclasts and ostracod grains. Beds are thin to medium (3–30 cm) in thickness and have gradational to sharp contacts with other grainstones.

The intraclasts are interpreted to have been broken and transported from carbonate mud flat areas that were partially lithified and dry. These clasts probably formed when a storm or sudden rise in lake level overtook these dried flats and ripped up the carbonate mud material, reworking the pieces to form well-rounded clasts or only moving the clasts short distances leaving them angular. These clasts also appear to have undergone dolomitization prior to their formation. This facies formed along near-shore and sublittoral areas in a moderate energy environment with other carbonate shoal deposits and adjacent to low energy carbonate sediments.

Lithofacies F7: Ostracod Lime Packstone-Grainstone

This lithofacies is an ostracod-bearing limestone with minor amounts of organic material and the rare oncoid (figure 6C).

Beds display massive, wavy, or plane-parallel laminations with grains oriented along laminations. Ostracod valves are closely packed, both broken and whole, and are commonly filled with dolomicrite. Ostracod grains commonly have minor coatings around shells and hold broken ostracod valve pieces inside a larger-whole shells intermixed with dolomite mud. Siliciclastic quartz, when present, is subangular to subrounded and silt sized. Organic material and fish scales display random orientations. F7 beds range from 2 cm to >1 m in thickness and are laterally continuous with sharp bases.

F7 represents a high energy environment with large grains and little mud. F7 is found in marginal to sublittoral areas. Finer-grained muds and silts were likely winnowed and redeposited in calmer environments. F7 beds are laterally associated with other carbonate shoal deposits and carbonate mudflats. These deposits are observed in core and outcrop where they are laterally adjacent to intraclastic packstones (F6), bioclastic packstones (F4) and interbedded with finely laminated oil shale (F18).

Lithofacies F8: Oolitic Lime Grainstone-Packstone

Lithofacies F8 is dominated by calcitic ooids with varying amounts of siliciclastic quartz, organic fragments, and ostracod shells. Beds are massive, plane-parallel laminated or wave-rippled (figure 6D) and ooids are sub-spherical to spherical and superficial. Ooid cores vary in composition and include ostracods, peloids, quartz grains, or host intraparticle porosity. Grains are closely packed and range in size from 0.5 to 2 mm, with a median size of 1.25 mm. F8 is typically associated with ostracod fragments that are lightly coated with calcite and range in size from 0.5 to 1 mm. Intraparticle and oomoldic porosity are dominant in the 1 cm- to >1 m-thick beds that are moderately continuous laterally and have sharp basal contacts. F8 is primarily observed in outcrop.

This facies is interpreted to have been deposited in a high-energy littoral environment. Ooid grainstones possibly formed near an inlet for fluvial systems or areas influenced by wave and wind activity in areas along the eastern margin of Lake Uinta. These deposits accumulate where wave energy and precipitation of carbonate are active in the water column. F8 is a carbonate shoal and occurs laterally adjacent to carbonate mudflat deposits.

Lithofacies F9: Oncolite-Ooid Lime Packstone-Grainstone

Lithofacies F9 is dominantly composed of oncoid grains that have irregular, micritic concentric laminations mixed with ooid grains characterized by even, concentric laminations (figure 7A). The irregular micritic laminations are thought to result from microbial-induced precipitation of calcite. Grains commonly possess both types of laminations. Oncoid-ooid grains are commonly mixed with ostracods, molluscan fragments, and microcrystalline lime mud. Beds show overall lack of structure and are thin from a few cm to 10 cm thick. Grains are ellipsoidal to sub-spherical in shape and range in size from 2 to 6 mm in diameter. Grain nuclei are composed of ostracods, peloids, bivalve fragments, and quartz grains. Porosity is interparticle, intraparticle, intercrystalline, and oomoldic. Beds were generally locally deposited and are not laterally continuous.

F9 is formed through microbial induced precipitation of calcite. These deposits are subrounded and are interpreted to form in episodic wave action that partially rounded the grains. Grains accumulate in partially restricted areas and are intermixed with ostracods.

Lithofacies F10: Ooid-Pisolite Lime Packstone-Grainstone

Lithofacies F10 is dominantly composed of pisoid grains >2 mm and peloid grains with varying amounts of ostracod fragments, molluscan shells, and microcrystalline dolomite (figure 7C). Beds are massive to plane-parallel or wavy laminated, though a lack of structure is most common. Pisoids are subspherical to spherical in shape and range in size from 2 to 4.5 mm in diameter. Pisoid cores are composed of ostracods, peloids, shells, and quartz grains. Porosity is interparticle, intercrystalline, and moldic. F10 beds are very thin to thin (1–10 cm) with gradational bed contacts. Beds are local deposits and not laterally continuous.

This facies formed in lower energy environments than ooids, but higher energy than the carbonate flat muds. The grain support fabric of these pisoid grains suggests episodic energy to move grains and allow coating to precipitate. These deposits accumulated in areas along shorelines extending offshore into a few meters of water depth. F10 is laterally adjacent to carbonate shoal grainstones (F7, 8, 9, 11), which formed in high energy environments, and carbonate mudflat (F2) deposits, which accumulated in low energy environments. This facies is primarily observed in outcrop.

Lithofacies F11: Bioclastic Lime Floatstone to Rudstone

Facies F11 is a molluscan, ostracod-rich crystalline limestone with varying amounts of siliciclastic quartz grains and organic material (figure 7B). Beds in this facies grade from a floatstone to a rudstone lacking mud and show wavy to structureless bedding. The bivalve and ostracod shells present are both broken and whole, and range from 2 to >25 mm in size, with the average grain about 5 mm. Siliciclastic quartz grains are minor and range from very fine to fine sand and are angular to subangular. F11 beds are thin (1–10 cm) and have both gradational and sharp basal contacts.

F11 is a high-energy deposit. The gradational contacts and chaotic nature of these beds supports a storm or singular event

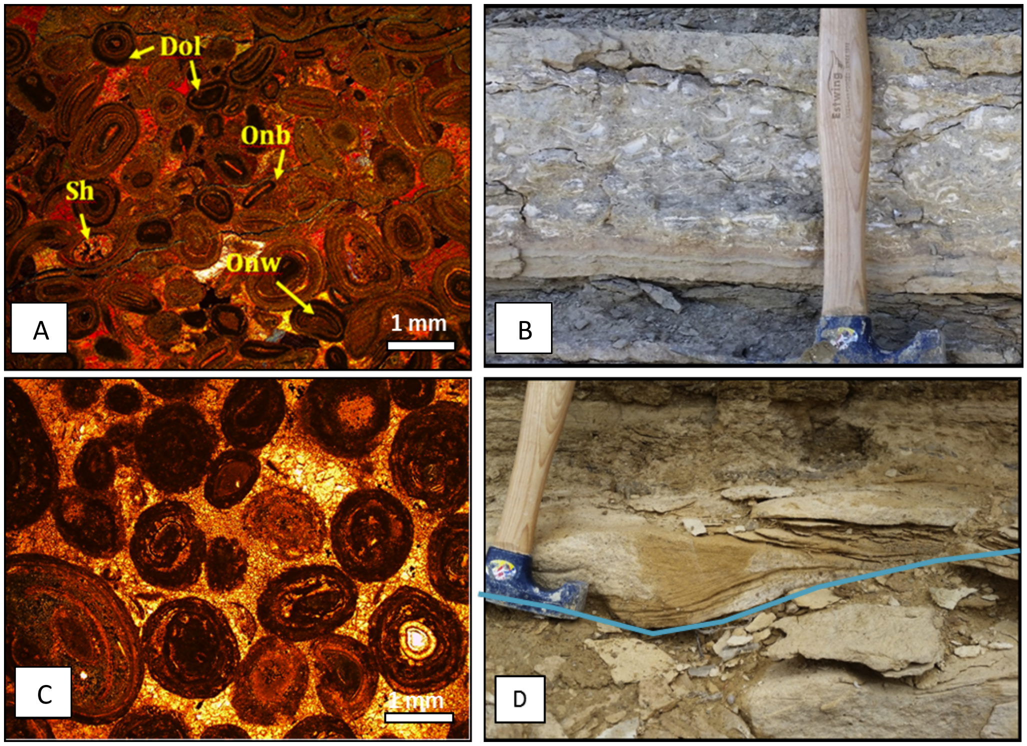

Figure 7. A. *F9 oncolite lime packstone-grainstone with broken ostracod shells (Onb) and whole ostracod shells (Onw), shelter porosity (Sh), and dolomite mud (Dol) (Texas Creek 2, sample #15, PPL). Blue epoxy shows pore space in B and E;* ***B.*** *F11 bioclastic lime floatstone to rudstone with bivalves (Hells Hole 3);* ***C.*** *F10 ooid-pisolite lime packstone-grainstone with ostracod shells (Hells Hole 2);* ***D.*** *F12 ostracod bearing sandstone (Missouri Creek 2).*

deposit. These coarse grainstones are found in distal littoral to sublittoral regions of the lake, primarily down-dip from an area rich in packstones and grainstones where oxygen levels are high and biota flourish. F11 is associated with illitic oil shale (F16), littoral to sublittoral siltstones (F1), and argillaceous dolomudstone (F17).

Lithofacies F12: Ostracod Bearing Sandstone

Lithofacies F12 is an ostracod-bearing, fine- to medium-grained quartz sandstone with varying amounts of detrital grains (clay and feldspar) and organic material. Beds are thin to very thick (3–100+ cm), well sorted, and contain varying amounts of ostracods. They are current ripple cross-laminated or are massive. The quartz is well sorted, subangular to subrounded, ranges from fine to medium grain size, and is well sorted. Ostracod grains are whole or broken and occur in thin bands within the sandstone beds. This facies occurs in limited locations on the eastern margin of the study area (figure 7D).

The ripples in this facies suggest a high energy environment along the margin of the lake. This sand could also be from deeper littoral to sublittoral regions of the lake deposited offshore during storm events when high wave energy was present. The sand was transported into the system through rivers and streams from the Douglas Creek Arch just a few kilometers to the east. These beds are laterally adjacent to carbonate shoal deposits and littoral to sublittoral siltstone deposits.

Lithofacies F13: Structureless to Laminated Sandstone

Lithofacies F13 sandstone beds are fine to medium grained, quartz-rich with varying amounts of feldspar and plagioclase (figure 8A). Grains are angular to subrounded and poorly sorted. Beds are structureless to laminated and laterally continuous in outcrop with no channelization or change in bed thickness over tens of meters. F13 bed contacts have sharp bases.

Facies F13 represents sediments which were probably deposited as distal stream mouth bars along the lake margin. Sediment inputs were from local river systems during periods of high discharge. These beds are associated with littoral to sublittoral siltstones and illitic oil shale and occur in littoral to sublittoral depositional environments.

Lithofacies F14: Cross-Stratified Sandstone

Lithofacies F14 is fine- to medium-grained, well-sorted, tan to yellow sandstone with half-meter scale cross-stratified laminations, cut and fill structures, and current ripples (figure 8B). This facies forms within a sandstone unit that has a sharp base and is channelized. This unit locally occurs in association with green-grey siltstones and claystones and laminated sandstones. This sandstone filled channel can be traced for 30 meters to both edges of the channel body.

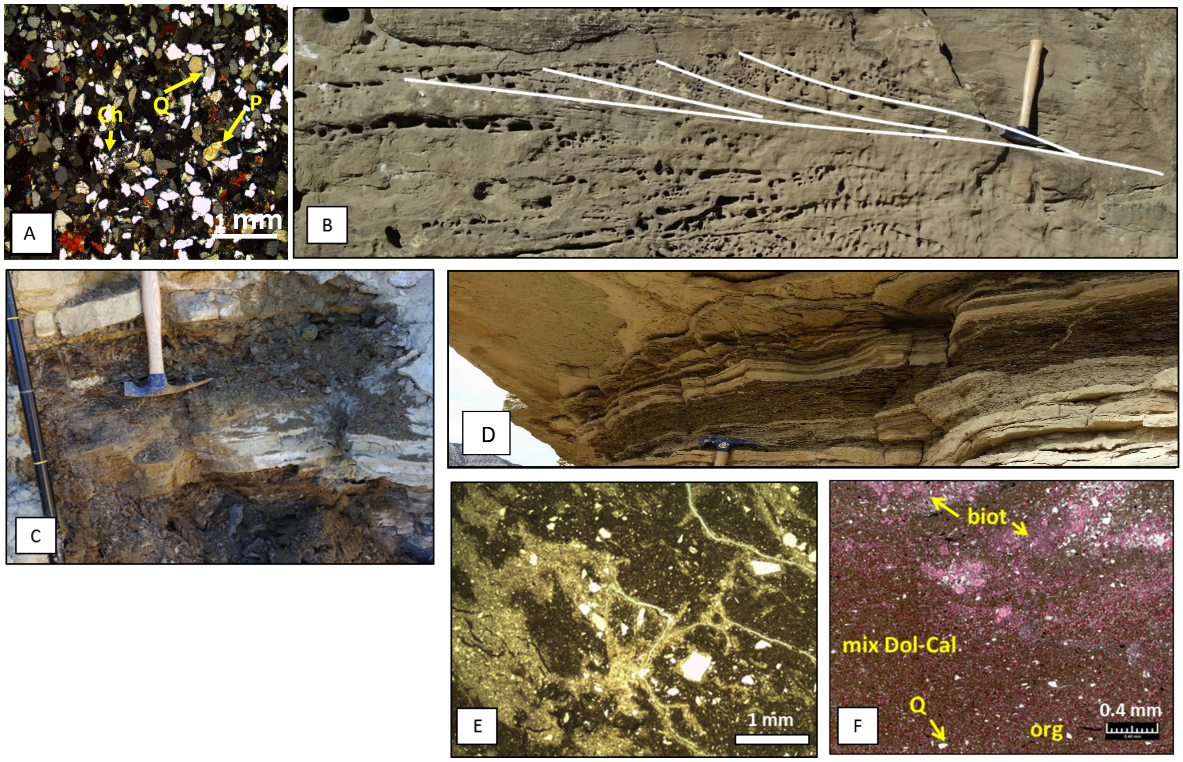

Figure 8. A. *F13 structureless to laminated sandstone, Ch-chert, Q-quartz and P-pyrite (Texas Creek 2);* ***B.*** *F14 cross-stratified sandstone (Evacuation Creek 3);* ***C.*** *F15 carbonaceous shale (Texas Creek 2);* ***D.*** *F16 laminated illite claystone (Missouri Creek 2);* ***E.*** *F17 argillaceous mudstone with micrite and angular quartz grains (white), (Texas Creek 1);* ***F.*** *F18 laminated silty oil shale, containing possible bioturbation (biot), lime mud (Dol-Cal), organic material (org), and silt size quartz (Q), sample from Anadarko NBU 921-22M core, photomicrograph prepared by Weatherford Labs.*

Facies F14 cut and fill features, ripples, and cross-stratification represent a high energy directional system. The well-sorted material suggests that sand was transported over some distance. This facies is interpreted as fluvial channel-fill sediment that fed into the basin.

Lithofacies F15: Carbonaceous Shale

Facies F15 is a thinly laminated organic accumulation. This bed is tabular, 10 to 20 mm thick, and rich in plant material and organic fragments (figure 8C).

This facies represents a backwater environment that was not in the main lake body, but just outside of the lake along the shoreline. This facies represents a swamp environment that likely formed in quiet, protected areas along the lake shore.

Lithofacies F16: Laminated Illitic Claystone

Lithofacies F16 is distinguishable by brown and tan color in outcrop and is a dolomitic clay-rich deposit dominated by illite, montmorillonite, and chlorite clay (QEMSCAN® results, see Calcite, Dolomite, and Porosity section below). This facies is parallel-laminated and sheet-like in geometry (figure 8D). Clay beds, intermixed with thin dolomite layers, are lean in organic content. Rare ostracods are associated with these units. Beds are thin to medium in thickness (3–30 cm) and occur in the upper portion of the Uteland Butte member in the Missouri Creek area along the eastern margin of Lake Uinta.

F16 is a distal littoral to proximal sublittoral deposit that is relatively rich in kerogen compared to surrounding facies, but lean compared to the sublittoral oil shale from the distal cores. This facies represents a low energy environment that received sediment probably through suspension from the water column. F16 is laterally adjacent to bioclastic lime floatstone and rudstone deposits (F11), and argillaceous mudstones (F17).

Lithofacies F17: Argillaceous Mudstone

Lithofacies F17 is a calcareous mudstone with ostracod shells, minor amounts of authigenic calcite, and siliciclastic grains (figure 8E). These beds show fine parallel-laminations that are rich in organic material. Ostracods found in F17 consist of fragments that show minor variability in orientation and are locally concentrated within dolostone (<3 cm thick). Horizontal burrows are present. Silt grains often occur in lenses and range in size from very fine to coarse silt and are subangular to subrounded. F17 bed thickness ranges from 2 mm to >1 m and contacts are sharp or gradational.

This facies represents a moderate energy depositional environment that experienced increased siliciclastic input. The facies likely occurred in a more proximal sublittoral environment than the laminated oil shale (F18) and closer to the siliciclastic input areas. F17 is also associated with ostracod and mollusk wackestones (F3 and F4) and ostracod packstones (F7). This facies is only observed in cores.

Lithofacies F18: Laminated Silty Oil Shale

Facies F18 beds are aphanocrystalline to very fine crystalline, authigenic dolomite that has replaced an original calcareous and clay-rich matrix (figure 8F). These kerogen-rich beds have parallel-laminations which are dominantly matrix-rich with a few grain-rich laminations. Rare, small, horizontal burrows occur within F18. Sparse siliciclastic grains within these beds are subangular to subrounded and range in size from fine silt to fine sand. Beds have sharp, discontinuous contacts which occasionally host load structures and are 3 mm to >1 m thick.

F18 is a low energy facies that represents a depositional environment supplied with sediment from suspension fall-out and precipitation from the water column. These beds are far from fluvial influx. F18 is found in the distal-sublittoral to shallow profundal area of the lake where anoxic conditions preserve the kerogen-rich beds and where bioturbation from organisms is rare. This facies is only observed in core.

FACIES ASSOCIATIONS

The Uteland Butte sedimentary facies (F) as defined by sedimentary structures, textures, and composition are grouped into eight facies associations (FA) based on lateral and vertical relationships (table 2). Facies associations are grouped into lacustrine environments or zones based on energy level and relative water depth. During deposition of the Uteland Butte member, Lake Uinta consisted of littoral, sublittoral, and perhaps shallow profundal environments.

Littoral deposits, observed mainly in outcrop, are rich in siliciclastic and carbonate material. Siliciclastic deposits are predominantly fluvial sandstone to littoral and sublittoral siltstones characterized by low-angle cross-stratification and plane-parallel cross-stratification. These deposits are primarily found at the base of the Uteland Butte member. Deeper lacustrine zones rarely have thick silt and sand accumulations.

Laterally continuous carbonate shoal facies persist along the eastern margin of Lake Uinta. Shoal deposits vary widely in thickness, have sharp bases and are rich in ostracods, dolomitic intraclasts, oolites, oncoids, and bivalve shells. These deposits are typically interbedded cyclically with littoral siltstones. Microbial carbonates are rare and occur as 2 to 3 cm thick capping deposits on ostracod and intraclast grainstones.

Littoral to sublittoral oil shale deposits occur in outcrop in the upper portions of the Uteland Butte member and in association with littoral to sublittoral siltstones and littoral to sublittoral bioclastic mudstone to wackestone deposits.

Sublittoral deposits were observed mainly in core. These beds are mostly bioclastic-rich packstones and wackestones and laminated deposits of littoral to sublittoral oil shale that show large variations in kerogen content.

Facies Association A: Fluvial-Deltaic Deposits

Facies Association A (FA-A) is a fluvial-deltaic deposit containing mixed channel-form sandstones with cross-stratification and scour and fill (F14), as well as structureless sandstone (F13) (figure 9). Color ranges from light tan to yellow or grey-black. F14 bodies vary in thickness from 2 to 5 m and contain concave-up scours, no bioturbation, climbing ripples, high-angle cross-stratification, and plane-parallel laminations. In places, F13 sandstones are bioturbated and contain ostracod shells. Sandstone deposits are laterally discontinuous and the average width is around 15 m. Sand bodies are associated with grey/green siltstone (F1) and have medium to fine-grained subangular clasts that are well sorted. Channel orientation indicates flow from the east and southeast.

The presence of ostracods and moderate sorting of subangular grains of medium to fine sand in the large channel deposits suggest a locally sourced fluvial channel deposit that formed at the edge of a standing water system (Schomacker and others, 2010). Downstream fining is suggested from tracing the channel fill deposit outcrop (figure 9A) in the lakeward direction (figure 9B). The velocity of the discharge in this channel dropped significantly upon contact with a water body the size of Lake Uinta, depositing medium- to coarse-grained material along the shoreline and finer grained sediments in more distal regions.

Areas with large delta influence show increased amounts of sand and silt deposition and less carbonate shoal accumulation. These deltaic deposits were dominantly sourced from the southeast near Evacuation Creek. Minor fluvial influence was observed to the north in the Texas Creek area and no large sand deposits were identified in the northern Hells Hole Canyon area. FA-A is not present in the cores.

FA-A is overlain by ostracod grainstones (F7) and grey/green siltstones (F1) that are interbedded with dolomitic pelodial mudstones (F2) and bioclastic wackestone (F5).

Facies Association B: Shoreline Carbonate Mudstones

Shoreline carbonate mudstones (FA-B) consist of fine-grained micritic to dolomicritic mud associated with calm, oxic water conditions (figure 10). This facies association commonly

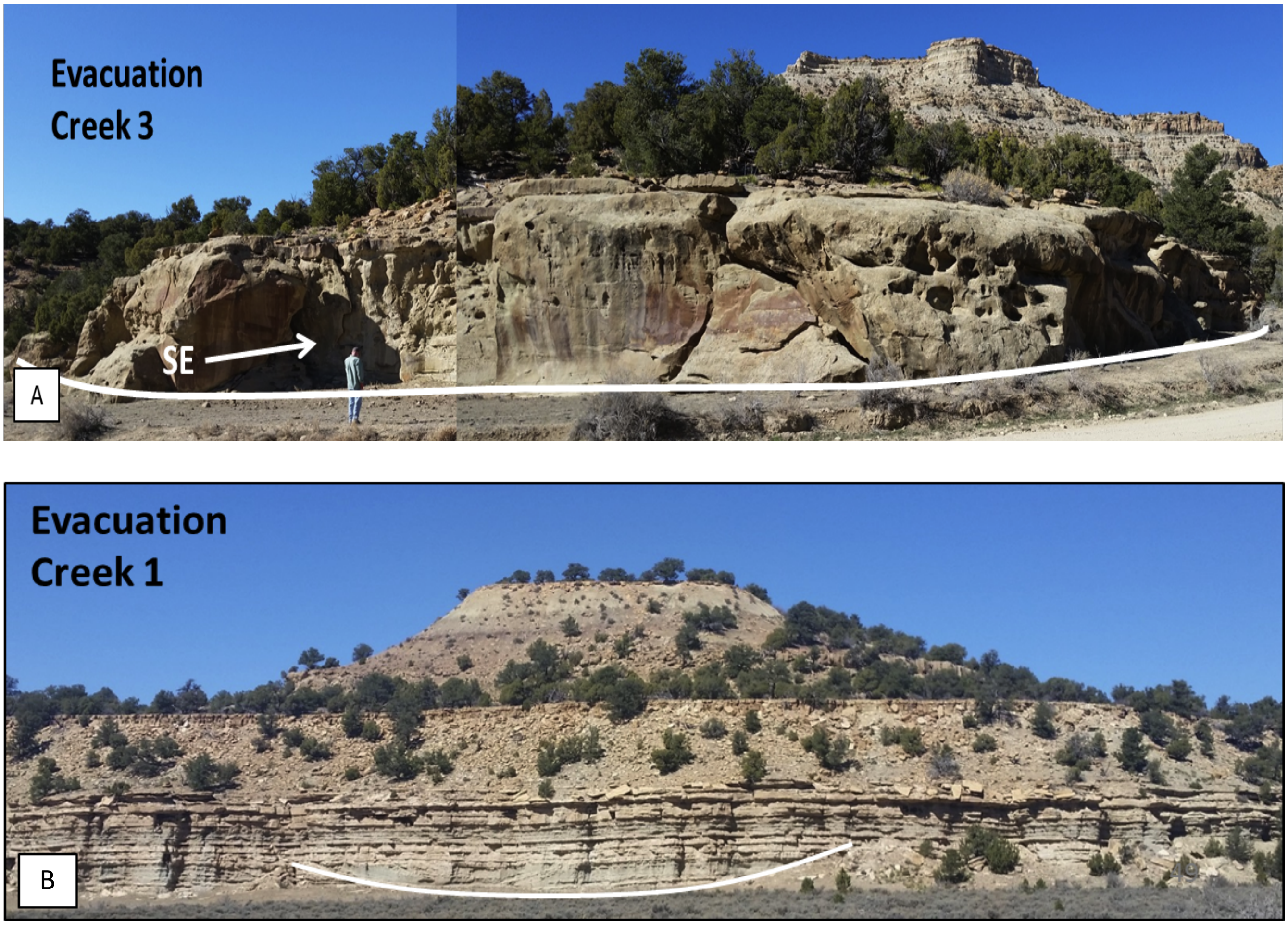

__Figure 9.__ Facies Association A. __A.__ Channel body in middle Uteland Butte in southern Evacuation Creek; the channel is 30 m wide and 6 m high; __B.__ F1 grey/ green siltstone and thin F13 structureless to laminated sandstones filling channel farther lakeward of (A).

contains ostracods and is found along the shoreline (figure 10A, B, C, D) and extends into the deeper littoral and proximal sublittoral regions where oxic and low energy conditions are maintained.

This association occurs throughout the entire Uteland Butte member along the eastern portion of the Uinta Basin and in the cores farther to the northwest. These beds can be traced laterally hundreds of meters along the outcrop. FA-B occurs interbedded with carbonates composed of floatstone to rudstone, grainstone to packstones, and carbonate mudstones that are structureless or contain cross-stratification, ripple cross-lamination, and horizontal lamination. Grains include oolites, pisolites, oncoids, encrusted intraclasts, and bioclasts.

FA-B includes calcareous dolomitic mudstone (F2) (figure 10A, B, E), ostracod wackestone to packstone (F3) (figure 10C), molluscan mudstone to wackestone (F4), oolitic mudstone to wackestone (F5), and is associated with the grainstone facies (F6, F7, F8, F9). This facies association is also commonly found interbedded with fluvial-deltaic deposits (FA-A), littoral to sublittoral claystones to sandstones (FA-C), or carbonate shoals (FA-D).

Facies Association C: Littoral to Sublittoral Claystone to Sandstone

Facies Association C (FA-C) is a grouping of facies characterized by grey to green clay to silt size grains that are well sorted within homogeneous and laminated beds (figure 11A, B). Facies in this association include ostracod bearing sands (F12), grey/green siltstones (F1) (figure 11C, D), thin structureless sands (F13), and argillaceous mudstones (F17). Ostracods and preserved organic matter are common in these facies. Contacts are both gradational and sharp. Interbedded facies include calcareous mudstone (F2), ostracod, intraclast-ostracod and peloidal shoals (F6, F7, F8), and bioclastic wackestones (F3, F4, F5). Facies in this association contain burrows filled with carbonate material (FA-D) from overlying beds (figure 11E).

FA-C is genetically related to fluvial systems entering the basin carrying in siliciclastic sediment. This association is closely related to FA-A fluvial-deltaic deposits. FA-C sands represent a more distal sheet-like, down-dip deposit of coarser material. FA-C lacks wave modification features.

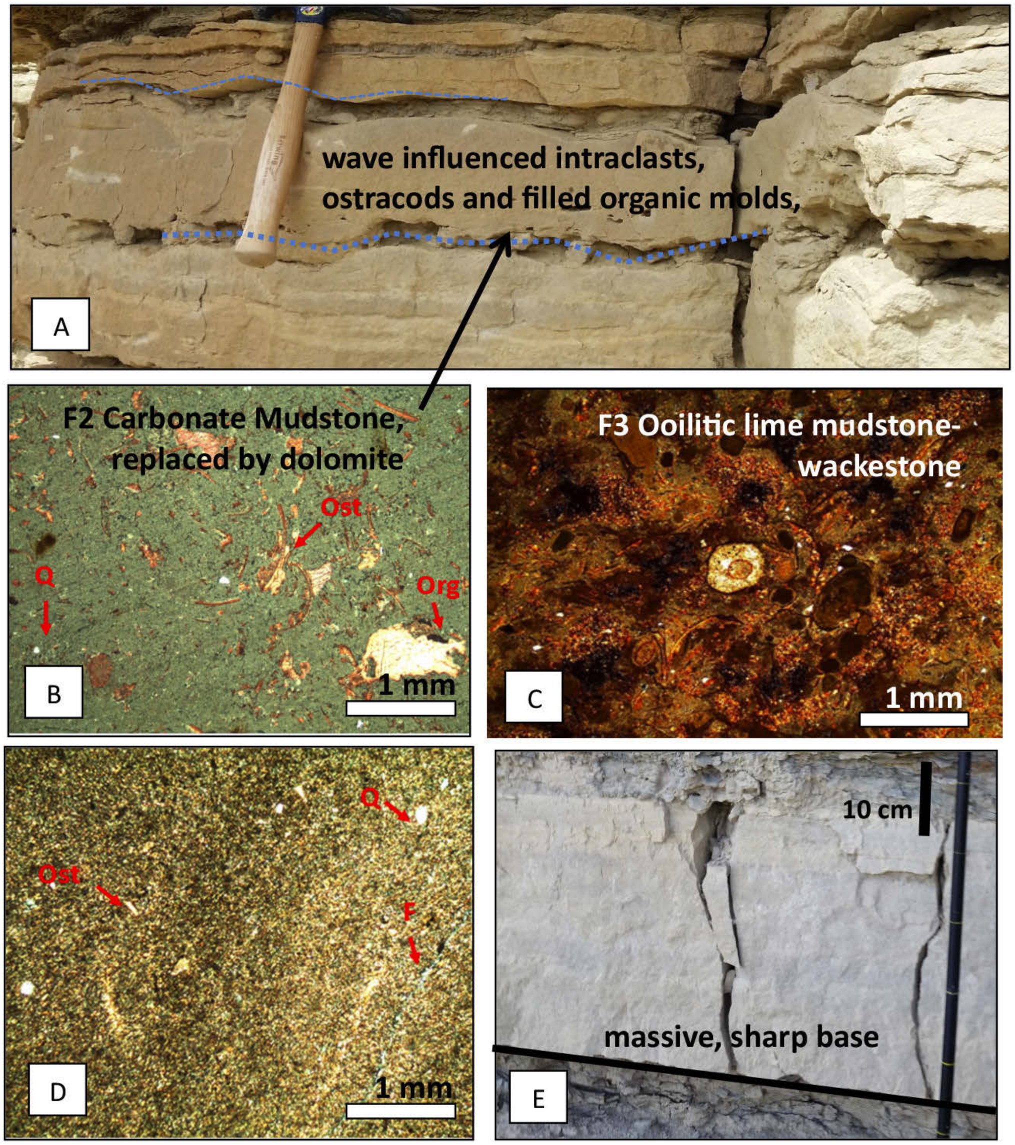

Figure 10. *Facies Association B.* ***A.*** *and* ***B.*** *F2 wave influenced lime to dolomitic mudstone with its associated thin section, Q-quartz, Ost-ostracod, Org-organic material from measured section CO 109, sample #5;* ***C.*** *F3 oolitic lime mudstone-wackestone that is a lens within a calcareous mudstone (Hells Canyon 2, sample #4;* ***D.*** *F2 lime to dolomite mudstone with quartz (Q), ostracod (ost), and fractures (F), (Evacuation Creek 2, sample #8);* ***E.*** *Sharp based F4 molluscan lime wackestone-packstone.*

Facies Association D: Carbonate Shoal

Facies Association D (FA-D) is a marginal littoral deposit of grainstones and packstones composed of oolites, oncoids, pisolites, ostracods, bivalves, and intraclastic carbonates (figures 7A, 12, and 13). Bioclasts and ostracods are the most common constituents. Sedimentary structures are present in the grainstones and packstones and include wave ripples, cross-stratification, and parallel lamination. Beds generally coarsen upward, range in thickness from millimeters up to 2 m, and are laterally consistent along the eastern margin of Lake Uinta (figure 12D).

This association is indicative of a high-energy depositional environment along the carbonate ramp in the littoral zone of the lake, typically accumulating in water along the shoreline. Pisoid and oncoid deposits are indicative of high energy, heavily reworked shallow-water areas of the littoral zone (Renaut and Gierlowski-Kordesch, 2010). This level of agitation is characteristic of shoal deposits and requires strong, persistent waves and currents. These are likely sourced from wind driven currents along the eastern margin of the lake. The presence of wave-rippled grainstones also indicates wave-influence along the lake margin. This association, in combination with FA-A and FA-B, can be used to approximate the shoreline geometry.

Shoals are usually interbedded with littoral to sublittoral claystones and sandstones (FA-C) and laterally associated with shoreline carbonate mudstones (FA-B) and fluvial-deltaic deposits (FA-A). FA-D deposits were formed in higher energy environments than FA-B, which is associated with calmer shoreline areas.

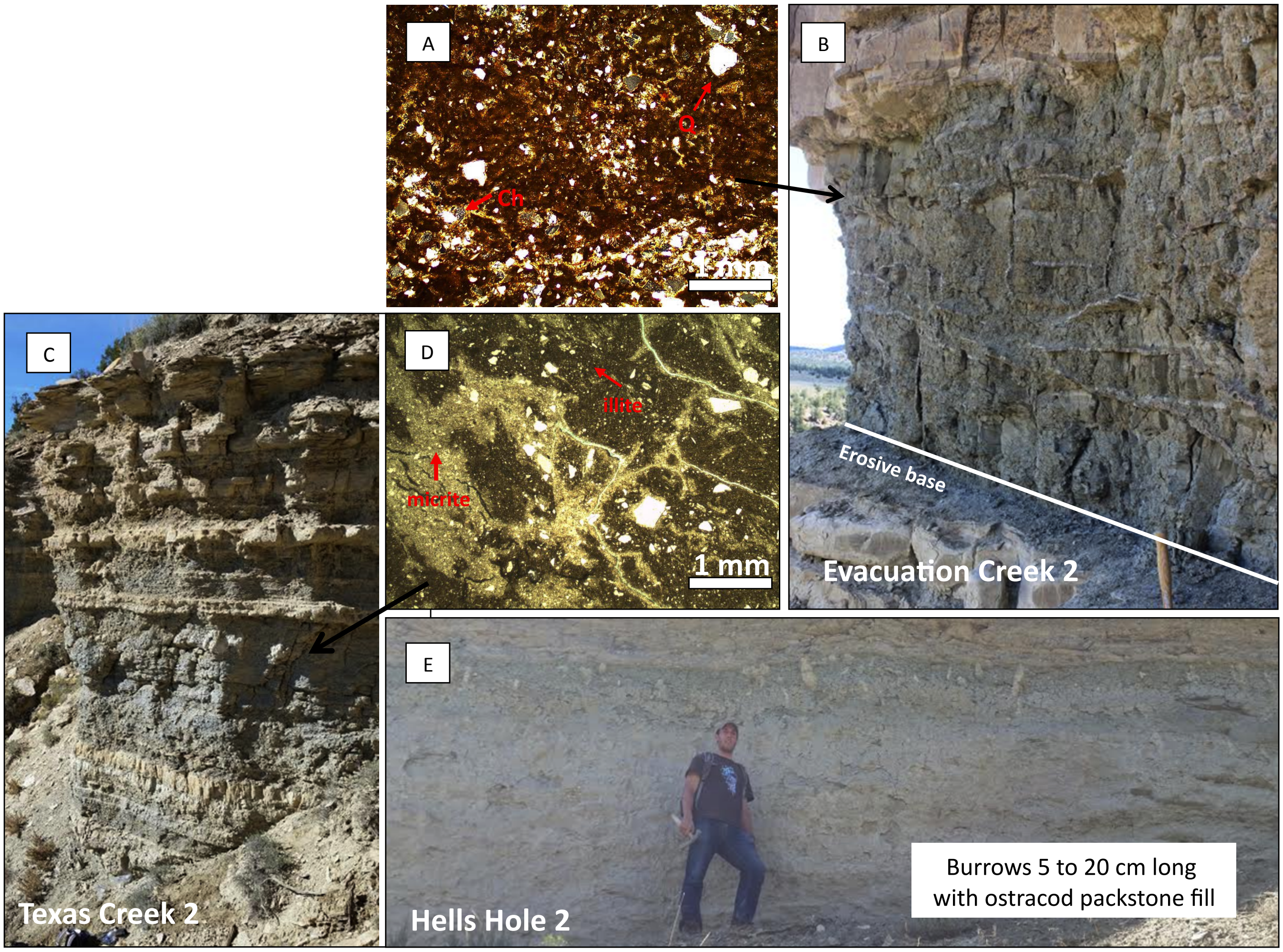

Figure 11. *Facies Association C.* ***A.*** *F1 faintly laminated grey/green-siltstone (F1) with subangular medium-sized quartz grains and chert (Evacuation Creek 2, sample #3);* ***B.*** *Thick grey/green siltstone (F1) bed with erosive base and gradational top, (Evacuation Creek 2);* ***C.*** *Outcrop with low net-to-gross, photomicrograph shown in (D) occurs along a transition zone between grey/green siltstone (F1) and calcareous mudstone (F2), (Texas Creek 2);* ***D.*** *F2 lime to dolomite mudstone with green silt, ooids, intraclast and subangular quartz grains, faintly laminated (Texas Creek 1, sample #3);* ***E.*** *grey/green siltstone (F1) burrowed at contact, burrows are 5 to 20 cm long and filled with the overlying ostracod packstone (Hells Hole 2).*

Facies Association E: Microbial Carbonates

The microbial carbonate facies association (FA-E) consists of minor growth in the form of very thin microbial films, oncoid packstones and grainstones (F9) (figures 7A and 14A, B, D), and within ostracod wackestone (F3) (figure 14C) observed in core and outcrop. These beds are thin, between one to ten centimeters, and occur in association with rip-up clasts and dolomite filled ostracod shells. Algal mat accumulation is wavy and made up of millimeter-size laminations visible only petrographically from core samples suggesting they accumulate in sublittoral lake regions. No dome features, heads, or well-developed biohermal mound features were observed. Overall the Uteland Butte member lacks microbial deposits. The poor development of microbial structures and the abundance of ostracods, bivalves, and gastropods suggest a freshwater lake containing consumers that prevented preservation.

Facies Association F: Littoral to Sublittoral Bioclastic Mudstone to Wackestone

Facies Association F (FA-F) consists of fine carbonate mudstones (F2), mollusk, intraclast, and ostracod wackestones (F2-F5), and argillaceous mudstones (F17) (figure 15). FA-F is characterized by light grey to tan brown beds that contain bioclastic material and are between centimeter and meter scale in outcrop and core. These units are interpreted to have been deposited in moderate- to low-energy depositional environments that occurred above the oxic/anoxic boundary within the littoral and sublittoral region.

FA-F occurs interbedded with littoral to sublittoral oil shale (FA-G), and littoral to sublittoral siltstones to claystone (FA-C). Vertically, FA-F is associated with FA-D and FA-E in more proximal littoral regions and associated with FA-H in the deepest region of the basin.

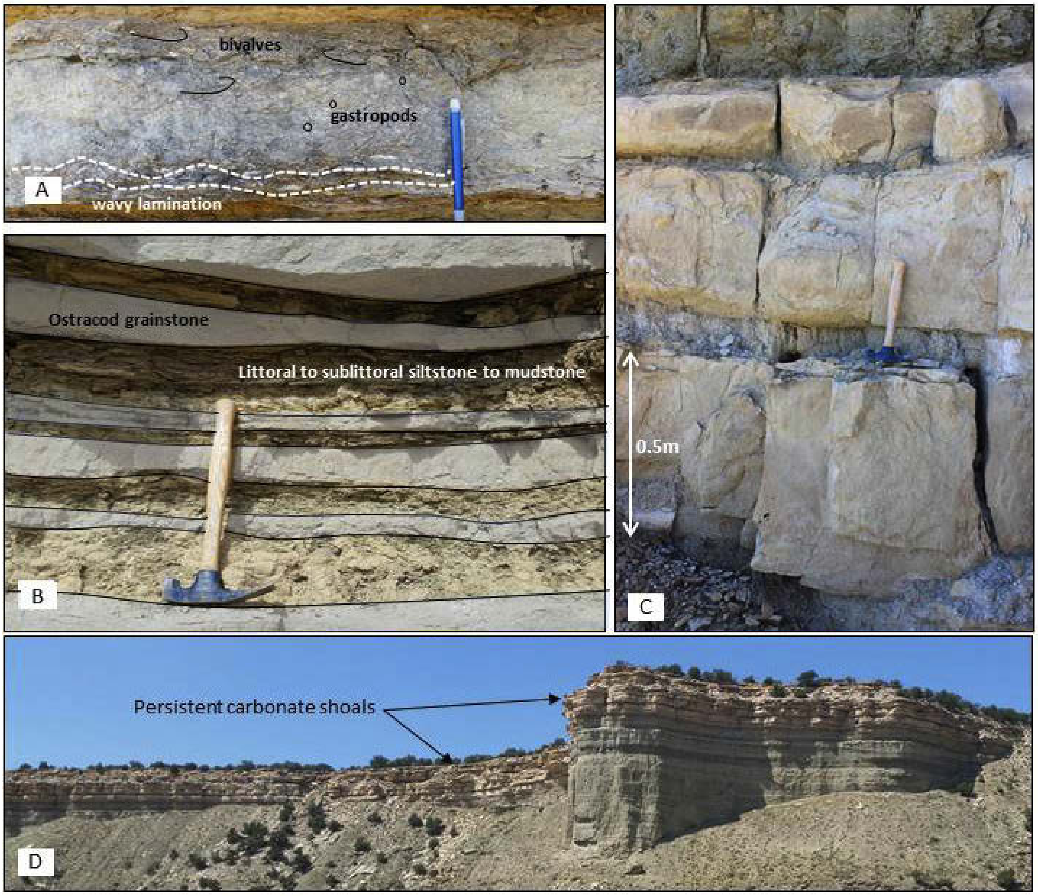

Figure 12. *Relationship of FA-C littoral to sublittoral mudstones to sandstones and FA-D carbonate shoal.* ***A.*** *Wave influenced bioclastic lime floatstone to rudstone (F11), 10 cm thick bed is contained within FA-C (Hells Hole 1);* ***B.*** *Thin, centimeter-scale cyclicity between FA-C and FA-D (CO109);* ***C.*** *Thick, meter-scale cyclicity between FA-C (recessive beds) and FA-D (thick, light tan beds) (Evacuation Creek 2);* ***D.*** *Persistent beds of FA-D across the outcrop in the uppermost Uteland Butte member, view to west towards the Hells Hole 3 (HH3) outcrop.*

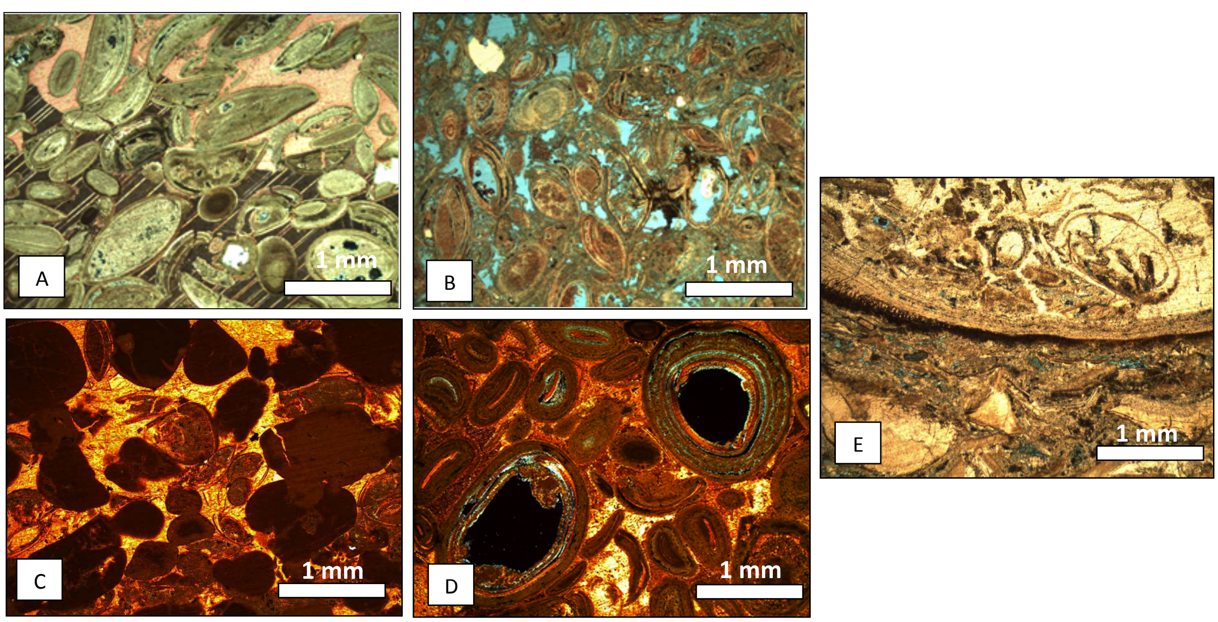

Figure 13. *Facies Association D.* ***A.*** *Ostracod lime packstone-grainstone (F7) with isopachous calcite cement and dissolution porosity (CO109, sample #17, XPL);* ***B.*** *Coated ostracod lime packstone-grainstone (F7) with inter and intraparticle porosity (CO 109, sample #18, PPL);* ***C.*** *Intraclastic-ostracod lime packstone-grainstone (F6), (Evacuation Creek 2, sample #16, 4x PPL);* ***D.*** *Oolitic-lime packstone-grainstone (F8) with calcite cement and intraparticle porosity (Evacuation Creek 3, sample #17, PPL);* ***E.*** *Bioclastic lime floatstone to rudstone (F11), (Hells Hole 3 sample #18, PPL).*

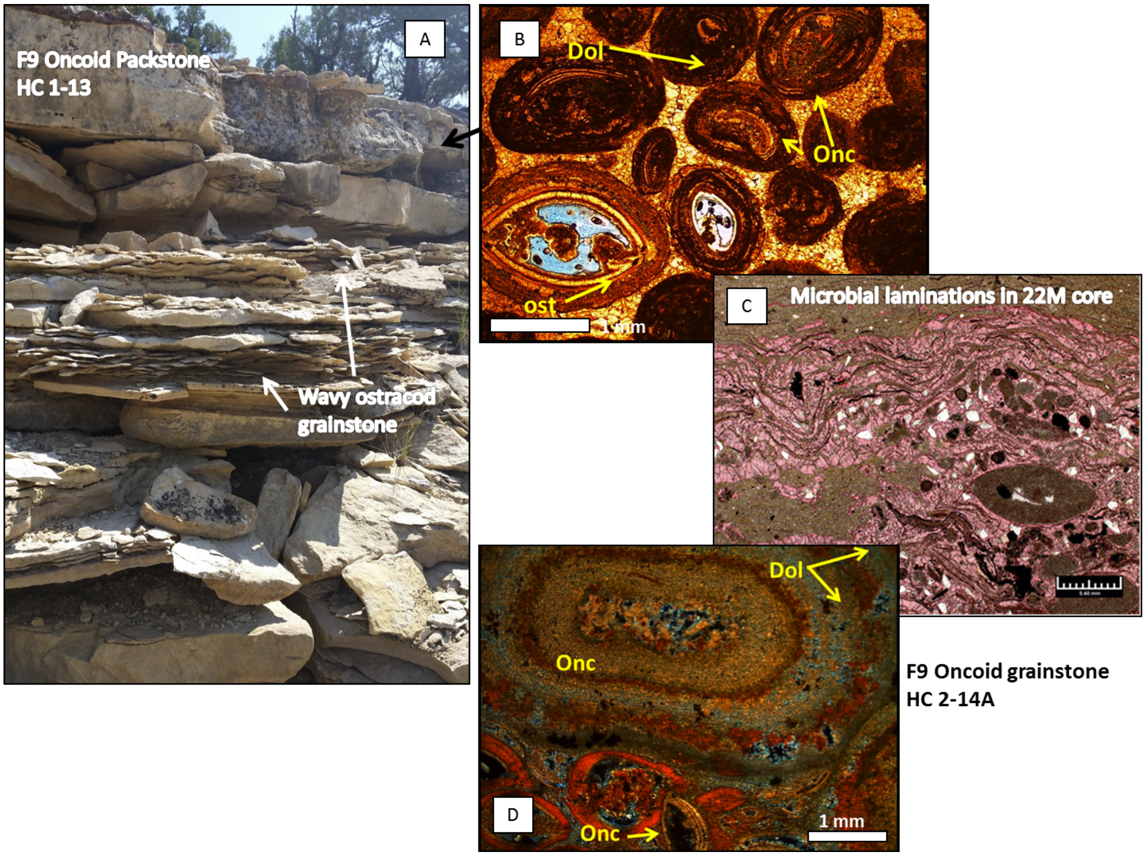

Figure 14. *Facies Association E.* ***A.*** *F9 oncolite lime packstone-grainstone in outcrop, unit is uniform thickness in outcrop and caps the top (Hells Hole 1);* ***B.*** *Photomicrograph of bed in (B), oncoid grains contain ostracod valves and are filled with lime mud (Hells Hole 1, sample #13);* ***C.*** *Microbial laminations in an ostracod lime mudstone-wackestone (F3) with subrounded silt grains, photomicrograph from NBU 921-22M core at 4907.6 foot depth. Black scale bar is 0.4 mm in length, photomicrograph prepared by Weatherford Labs;* ***D.*** *F9 oncolite lime packstone-grainstone; oncoid grain here is 5 mm in width (Hells Hole 1, sample #13).*

Facies Association G: Littoral to Sublittoral Oil Shale

Facies Association G (FA-G) consists of laterally laminated, organic-rich, illitic claystone (F16), laminated ostracod wackestone (F3), and argillaceous mudstones (F17) (figure 16). This oil shale is light tan to dark brown in color and is observed mainly in deeper lake environments, though it is also present in marginal to sublittoral areas. Fish remains and ostracods are commonly present in this facies association. Along the lake margin, organic richness is moderate to low. Beds are relatively thin in outcrop, about 0.5 m, and are thicker in the deeper subsurface deposits, about 2 m.

This association is interpreted as a low-energy environment in the distal littoral to sublittoral regions where oxygen levels are low and bioturbation is rare. These organic-rich carbonate and silty oil shales and mudstones were deposited in a large range of depths along the ramp-slope with low wave energy (Renaut and Gierlowski-Kordesch, 2010). These units are interbedded with littoral and sublittoral claystones to sandstones (FA-C) and littoral to sublittoral bioclastic mudstones and wackestones (FA-F). Beds are associated with laminated oil shale (FA-H) deeper in the basin and sublittoral ostracod packstones (FA-D) towards the margin. FA-G is present in both core and outcrop.

Facies Association H: Laminated Oil Shale

Facies Association H (FA-H) is made up of finely laminated, organic-rich oil shale (F18) (figures 8F, 17). This association is only present in core and is interpreted to represent the deepest depositional environment in the study area. Color ranges from dark-grey to black and has a higher organic content than shale in FA-G, which is more argillaceous. This association is typically plane-parallel, and bivalve fossils are occasionally present. Beds are several centimeters to a half-meter thick.

FA-H is interpreted as a deep, open-water deposit in the profundal portion of the lake where plankton and algal production is high, macrofauna populations are low, and organic preservation rates outpace carbonate production (Ryder and others, 1976; Renaut and Gierlowski-Kordesch, 2010). This facies is laterally and vertically associated with littoral to sublittoral oil shale (FA-G), littoral to sublittoral claystones to sandstones (FA-C), and littoral to sublittoral bioclastic mudstones to wackestones (FA-F).

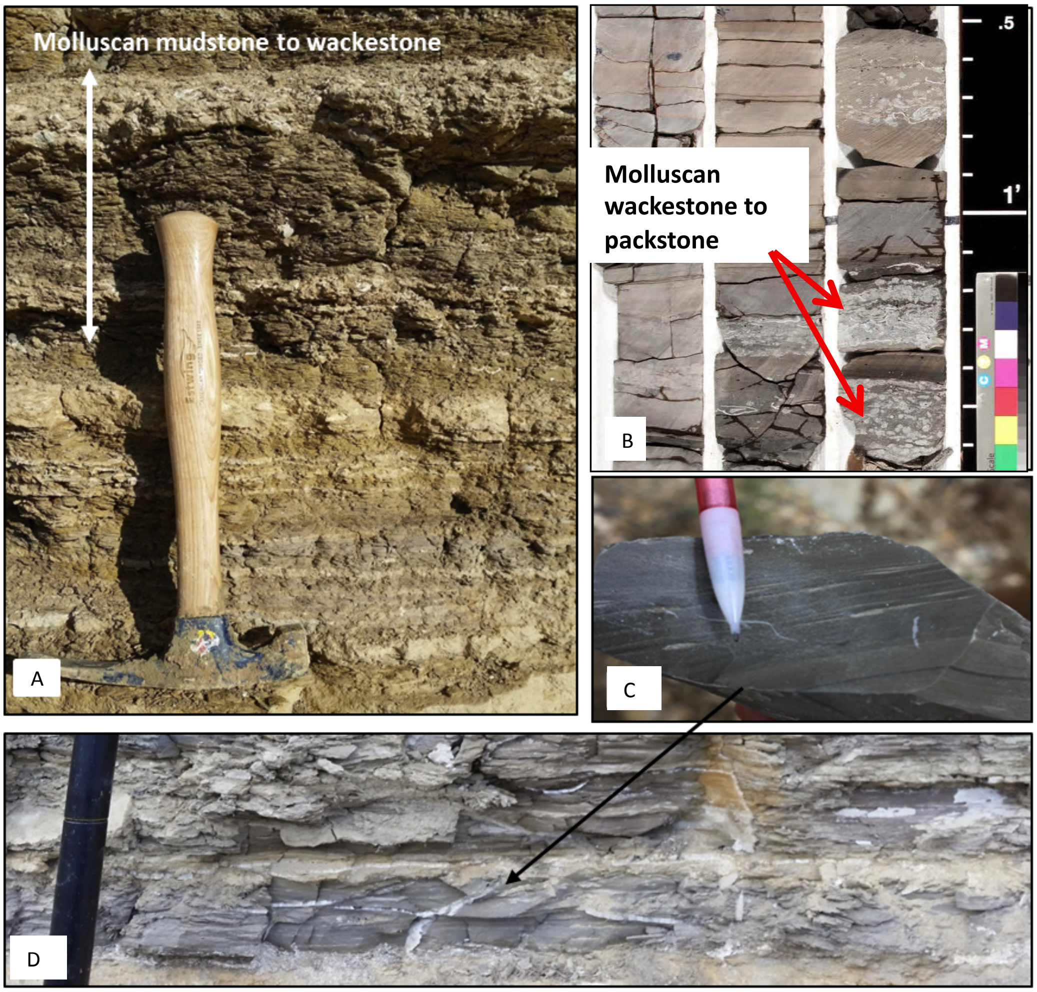

***Figure 15.** Facies Association F. **A.** F17 and F4 interbedded, argillaceous mudstone and molluscan lime wackestone-packstone (Hells Hole 1); **B.** F4 molluscan lime wackestone-packstone in NBU 921-22M core, 4870 to 4872.2 feet depth; **C.** Silt/sand lenses interlaminated with organic-rich mudstone (Evacuation Creek 1); **D.** Argillaceous grey-lime mudstone with silt lens (Evacuation Creek 1).*

DEPOSITIONAL MODEL AND SEQUENCE STRATIGRAPHY

The facies and facies associations described above were used to build a depositional model for the Uteland Butte member. The model illustrates the lateral distribution of the carbonate and siliciclastic facies extending from the ancient lake's southeast shoreline into the deeper part of the lake to the northwest (figure 18). Fluvial-deltaic (FA-A) and shoreline mudstones (FA-B) deposits are located in the backwater and shoreline area and are interbedded with lake units. The shoreline region of the lake is characterized by littoral to sublittoral claystones to sandstones (FA-C) that extend out into the basin and are interbedded with carbonate shoals (FA-D). Shoals containing ooids, pisoids, oncoids, and coated ostracod grainstones occur off axis from fluvial systems in areas with episodic waves and currents. Carbonate shoals (FA-D) also occur in deeper littoral environments where current energy is high. Carbonate shoals are commonly interbedded with littoral to sublittoral oil shale (FA-G), littoral to sublittoral bioclastic mudstones and wackestones (FA-F), and microbial carbonates (FA-E). These associations also interfinger with one another along strike. Farther into the deep sublittoral and profundal zones, organic-rich, laminated oil shale (FA-H) was deposited in a dysoxic to anoxic environment and interfingers with silty littoral to sublittoral oil shale (FA-G).

This depositional model was applied to measured sections and cores through analysis of thin section photos, bed character, and stacking patterns. A stratigraphic framework was compiled for each section to ensure consistency in interpretation before correlation. Figure 19 is an example of data from one outcrop, County Rd 109, with interpretations on lithofacies, facies associations, and stacking patterns. Facies were used to make interpretations about depositional environments and facies associations. The facies associations were used to predict the shallowing and deepening cycles of Lake Uinta—these cycles are represented as black (short-term) and red (longer-term) triangular cones. An example of these cycles is displayed on the outcrop image to the left of the measured section in figure 19. A lower, deeper littoral to sublittoral oil shale occurs interbedded with ostracod packstones, and this

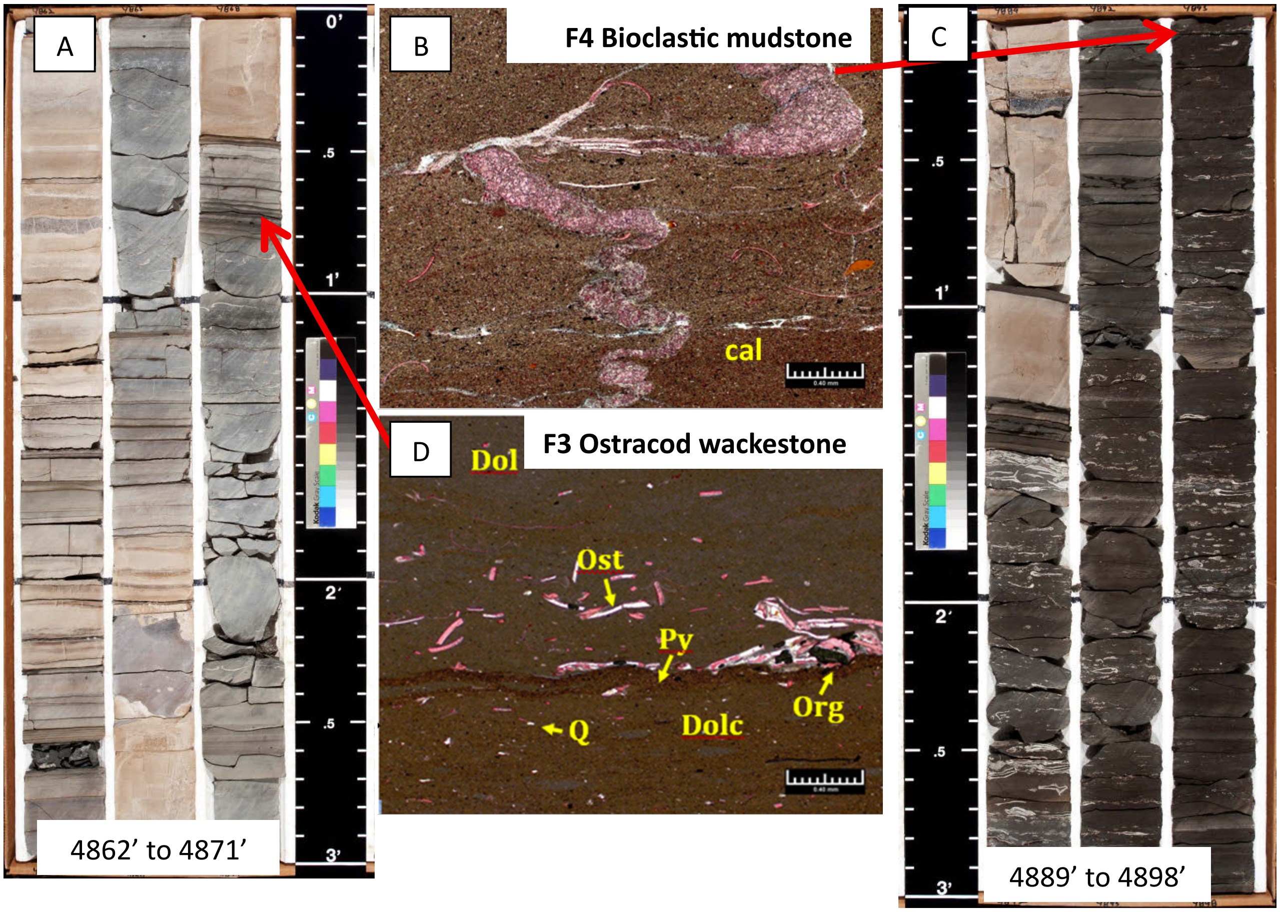

Figure 16. *Facies Association G.* ***A.*** *Core location of photomicrograph (D), this laminated ostracod lime mudstone-wackestone (F3) is interbedded with ostracod lime packstone-grainstone (F7), from 921-22M core at 4862 to 4871 feet depth;* ***B.*** *F4 molluscan lime wackestone-packstone with laminated mud (cal), organic material, and large compressed burrows, from NBU 921-22M core sample depth 4895.75 feet;* ***C.*** *Red arrow from (B) notes location of photomicrograph in NBU 921-22M core, F4 is dark grey, faintly laminated, and overlain by mollusk wackestones, sample depth 4889 feet to 4898 feet;* ***D.*** *F3 ostracod lime mudstone-wackestone, ostracod (Ost) grains concentrated in dolomitic mud laminations with organic material (Org) and pyrite (Py), 921-22M core sample depth 4868.65 feet; Black scale bars in (B) and (D) are 0.4 mm, photomicrographs prepared by Weatherford Labs.*

unit shallows upward into a mixed FA-D and FA-C littoral to sublittoral claystone to sandstone deposits and carbonate shoal. The section is capped by a thick carbonate shoal deposit (FA-D) (figure 19A-C). Figures 19D and 19E illustrate green grey siltstone (F1) and littoral to sublittoral oil shale (FG) that occurs at the base of cycles.

A sequence stratigraphic interpretation was constructed for the Uteland Butte member based on observations from this study and previous research completed by Cole and Picard (1978) and Little (1988). The framework shows a ramp lake environment for the Uteland Butte dipping westward into deeper Lake Uinta (figures 20 and 21). Shallow-marginal lacustrine environments are subject to episodic subaerial exposure, significant facies variations, and ultimately a very complex lateral and vertical facies-sequence history (Tucker and Wright, 1990; Platt and Wright, 1991; Bustillo and others, 2002). The stratigraphic interpretation presented below is based on facies association distribution, stacking patterns, organic richness of deposits, and depositional processes.

Littoral Lake Margin

Littoral to sublittoral siltstones and carbonate grainstone facies dominate in the shallow lake environment of Lake Uinta (figure 20). Shoal or shoreline grainstone facies reflect the wave and current energy in the lake system, which resulted in thick beds of abundant intraclast, ostracod, mollusk, and pelodial grainstones. Littoral carbonates grade laterally into floodplain or fluvial clastic deposits as energy changed along the shoreline. Carbonate facies were deposited in areas of low fluvial clastic input.

Figure 20 is a 20-km-long strike cross section along the eastern lake-margin of Lake Uinta, from Evacuation Creek in the south to Hells Hole Canyon in the north. The Uteland Butte is divided into four cycles based on significant flooding surfaces (dotted lines) at the top of overall shallowing upward cycles. The basal Uteland Butte contact is marked by an abrupt transition from Wasatch Formation paleosols to delta deposits, which represents the basal sequence boundary

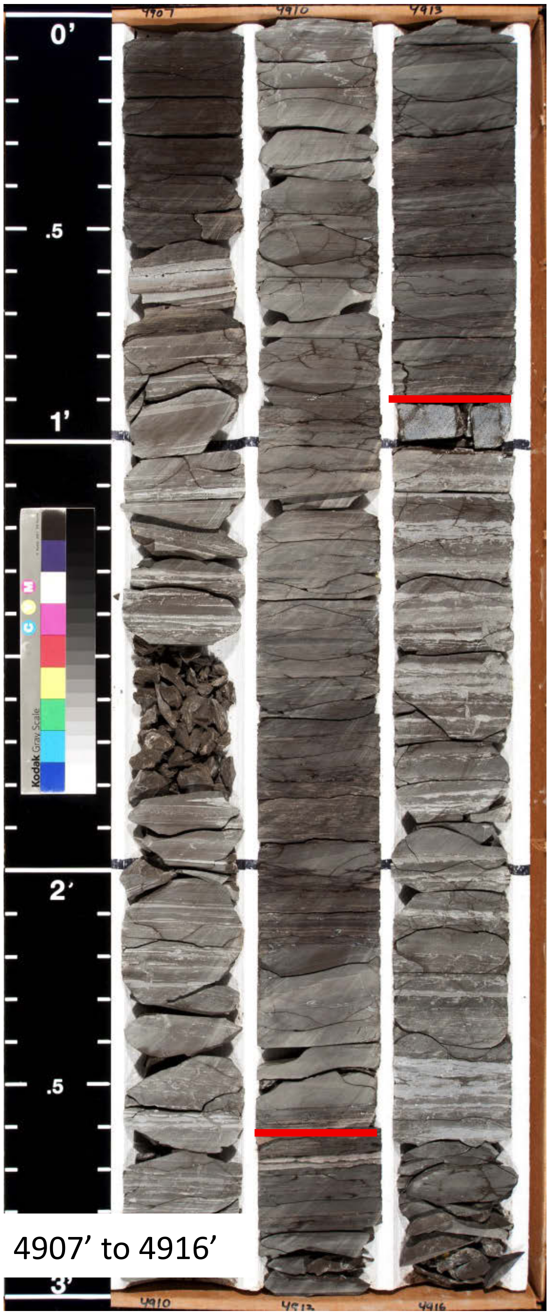

Figure 17. *Facies Association H. Black, laminated oil shale facies in NBU 921-22M core from 4907 to 4916 feet depth, between red bars.*

of the Uteland Butte in the study area. The basal delta sands have a uniform thickness where exposed in outcrop, contain ostracods, and show no channelization. These basal deltaic deposits signify an initial increase in runoff and early lake level rise (Tänavsuu-Milkeviciene and Sarg, 2012). As the lake continues to deepen, these delta deposits are overlain by littoral to sublittoral claystone to sandstone (FA-C). The lake then shallows upward through cycle 1 into carbonate shoals (FA-D) (section CO 109).

The base of the second cycle is marked by littoral to sublittoral claystones to sandstones (FA-C) and a thin rip-up-clast bed in Texas Creek 2 and Hells Hole 1. Second cycle ostracod packstones in the Texas Creek 1 and 2 outcrops contain notable amounts of quartz, indicating a nearby fluvial source and contributing to the thick littoral to sublittoral claystone to sandstone (FA-C) accumulations. Cycle 2 shallows upward into widespread carbonate shoal facies (FA-D) rich in mollusks, ostracods, and intraclasts.

Cycle 3 commences with widespread littoral to sublittoral claystone to sandstone (FA-C) and littoral to sublittoral bioclastic mudstone to wackestone (FA-F). The lake then shallows, depositing thick packages of ostracod shoals (F7, FA-D) at CO 109, Missouri Creek, and Hells Hole Canyon. This cycle contains the most continuous grainstone units and is richest in mollusks. These shoals are interbedded with thin accumulations of shoreline carbonate mudstone (FA-B) and littoral to sublittoral claystone to sandstone (FA-C). A large sandstone channel, six meters thick, is present in the Evacuation Creek area in cycle 3. This channel likely influenced the large quantity of silty accumulation seen in cycle 3 to the north.

The final flooding surface, the top of cycle 3, is marked by intraclastic rudstones in Evacuation Creek 3, CO 109, and Missouri Creek 1; by littoral to sublittoral oil shale (FA-G) in Texas Creek 1; and by littoral to sublittoral claystone to sandstone (FA-C) in Hells Hole Canyon 1 and Texas Creek 2. The Texas Creek 1 deposits above cycle 3 are littoral to sublittoral oil shale (FA-G) interbedded with intraclastic grainstones and coquinas (FA-D). Cycle 3, in the remaining sections is overlain by deeper littoral to sublittoral claystone to sandstone (FA-C), which gradually transitions into thick carbonate shoals (FA-D) that are interbedded in some areas with deeper littoral oil shales (FA-G), littoral to sublittoral claystone and sandstone (FA-C) (Texas Creek 2), and shoreline carbonate mudstones (FA-B) (Hells Hole 1). The carbonate shoal (FA-D) accumulations are thickest at CO 109 and Hells Hole Canyon 1 suggesting a lack of fluvial influence in these areas during cycle 4 deposition.

Sublittoral Lake

Uteland Butte sediments from deeper, open water lake settings are laminated; show some bioturbation; contain silt, ostracods and bivalve shells; and lack evidence of in situ vegetation (i.e., autochthonous coal). Figure 21 is a dip cross section correlating outcrops at Missouri Creek in the southeastern Uinta Basin to the NBU 921-22M core from the Greater Natural Buttes natural gas field to the northwest. The four outcrops in Missouri Creek are composed of FA-A fluvial-deltaic deposits, FA-B shoreline carbonate mudstones, FA-C littoral to sublittoral claystone to sandstone, FA-D carbonate shoals, FA-F littoral to sublittoral bioclastic mudstone to wackestone, and FA-G littoral to sublittoral oil shale. The core contains FA-C littoral to sublittoral claystone to sandstone, FA-D carbonate shoals, FA-F littoral to sublittoral mudstones, FA-G littoral to sublittoral oil shales, and FA-H laminated oil shales. Cycle

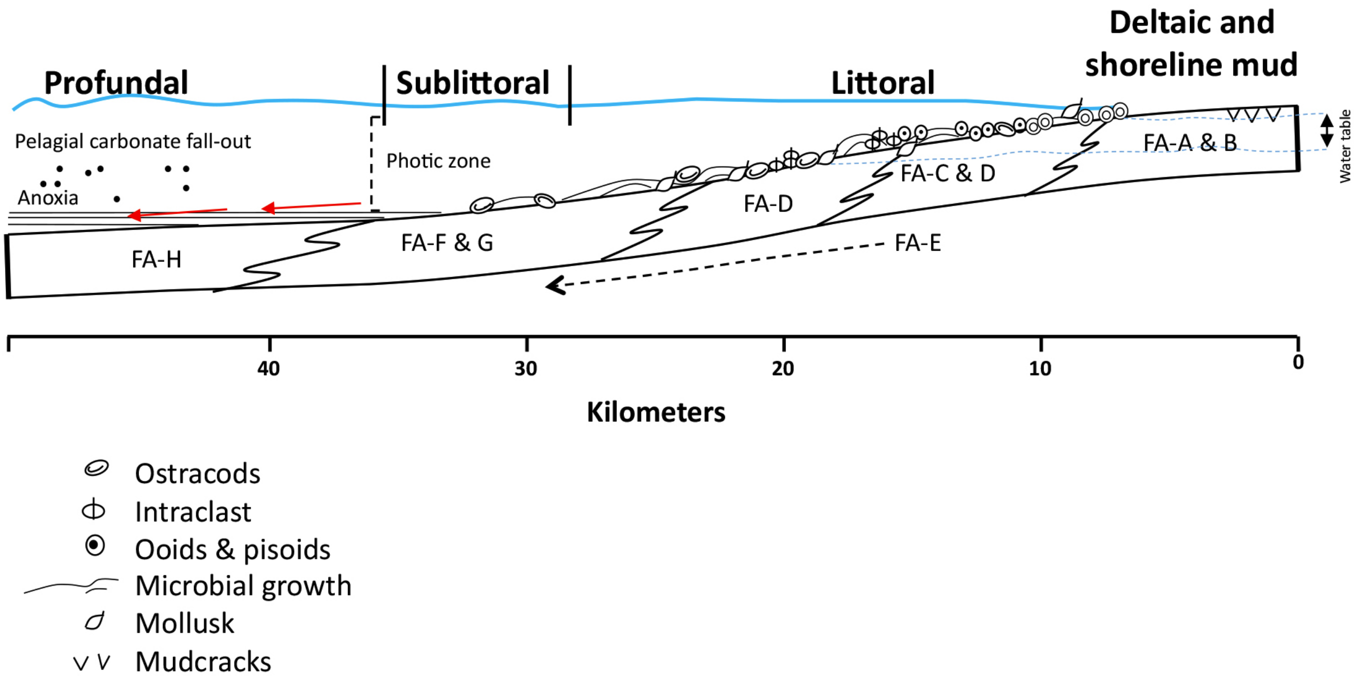

Figure 18. *Depositional model illustrating the lateral distribution of the limestone and siliciclastic facies associations deposited during Uteland Butte time in Lake Uinta's lacustrine (F1-F18) environment. The facies association distribution of the Uteland Butte member highlights the prominence of ostracods, intraclasts, peloids, and siltstones through the littoral and sublittoral regions. FA-E (microbial carbonate, dotted arrow below model) is minor and occurs in association with oncolite lime packstone-grainstone (F9) and ostracod lime mudstone-wackestone (F3).*

initiation was identified and correlated using rip-up lag deposits and the presence of deep lake oil shale facies overlying shallower facies. This cross section shows significant down ramp thickening and facies changes from lake-margin littoral environments in Missouri Creek to sublittoral mud-rich environments in the core. The basin core is dominated by the littoral to sublittoral mudstone to wackestone (FA-F) and littoral to sublittoral oil shale (FA-G).

DISCUSSION AND SUMMARY

The Uteland Butte member contains laterally persistent lacustrine lithofacies along the eastern basin outcrop area. The eastern edge of Lake Uinta was a gently dipping ramp (figures 20 and 21) subject to minor deltaic and fluvial influences, except in the Evacuation Creek area to the south. The outcrops display lake-margin, mixed siliciclastic and carbonate shoreline deposition composed of four major cycles. These cyclic deposits near the lake margin range from 3 to 7 m thick. Cycles are initially rich in sublittoral siliciclastic facies that shallow up to littoral carbonate shoals. Cycles 2 through 4 experienced similar regressions within each cycle where water levels were persistently in wave-dominated environments, but not proximal enough to accumulate terrestrial successions of clay or sand. In core, sublittoral cycle sediment accumulation ranges from as great as 3 to 12.5 meters. Laminated oil shale shallows upward into bioclastic wackestones and silty laminated oil shale in the sublittoral and distal littoral environment.

The fresh water environment of Lake Uinta hosted abundant populations of bivalves, gastropods, and ostracods during each cycle. The mollusk populations are particularly abundant to the north in Hells Hole Canyon where no fluvial influence was recorded. Hells Hole also hosted the thickest and most continuous successions of grainstones, with only minor thin units of silt. Mollusks are most abundant in the third cycle in the sublittoral areas, and it is possible that the third transgression was more nutrient-rich and fresher relative to other lake cycles.

Grainstone and packstone successions are prominent in both sublittoral and littoral settings, but the thickness of these beds are different. The thin, gradational and interbedded nature of the sublittoral packstones supports a different depositional process than the thick, meter-scale grainstones observed in lake-margin environments. The marginal grainstones also have a more laterally continuous nature within these facies over the entire 21 km N-S lateral transect studied. Although facies persist, lateral continuity of beds is not widely observed, as even outcrops that are only 0.5 km apart show little evidence to support bed-to-bed correlation. This is true for the two cores as well. Though the cores are located near one another, they do not display lateral continuity between grainstone and packstone beds. The sublittoral grainstones and packstones are possibly the result of high productivity during lake freshening periods when the deeper sublittoral to profundal lake environments were more oxic. In contrast, oxic fresh water persisted along the lake margin resulting in thick shoal deposits.

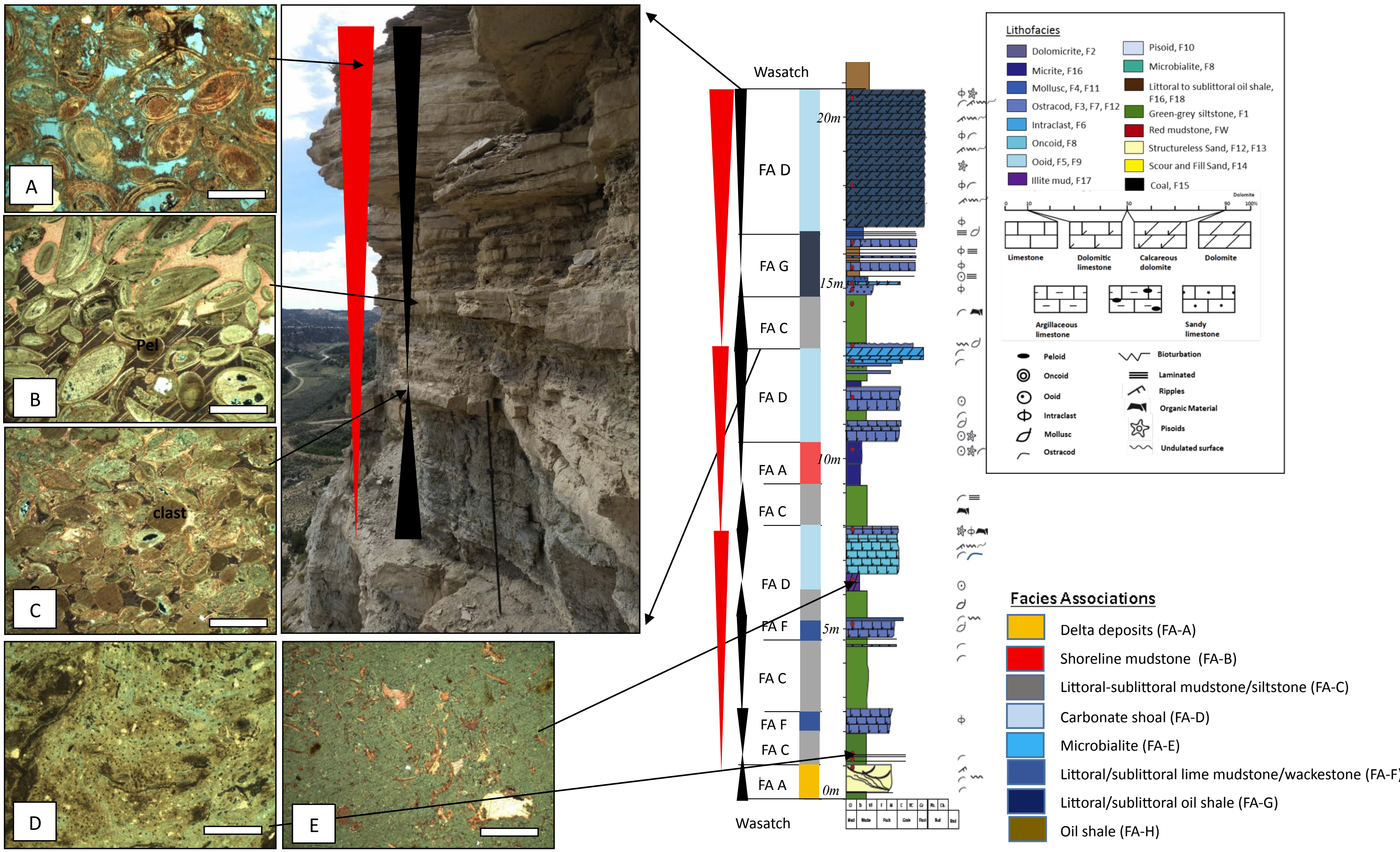

Figure 19. *Outcrop from CO109 measured section showing lithofacies and facies associations;* ***A.*** *F7 ostracod lime packstone-grainstone, with intraparticle and interparticle porosity, sample 18 (red dot on section) PPL 4x;* ***B.*** *F7 ostracod packstone, ostracod grains are coated, peloids (Pel), sample 17;* ***C.*** *F7 ostracod lime packstone-grainstone, sample 16;* ***D.*** *F1 grey/ green siltstone with quartz grains and micrite, sample 12;* ***E.*** *F2 lime to dolomitic mudstone, massive with ostracod valves, sample 5. Cones represent shallowing (widening upward) or deepening (narrowing upward) trends, red cones are lower order sequences and black are higher order cycles. Black rod in outcrop photo is 1.5 m long. Graphic section in middle shows facies associations on left and lithofacies on right. Grain size and carbonate texture scale for measured section, lower right.*

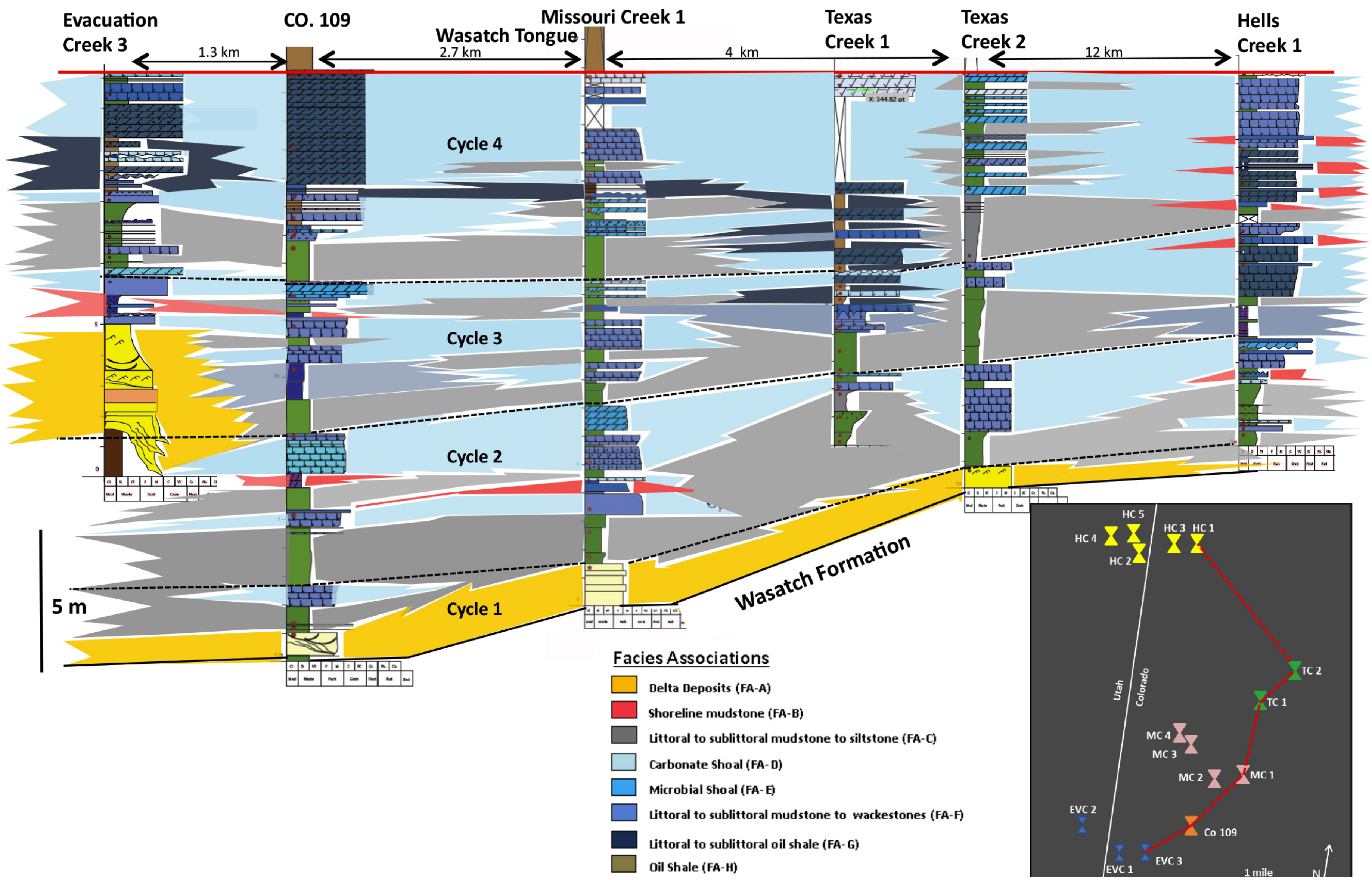

Figure 20. *Strike cross section along the eastern margin of Lake Uinta from south to north, Evacuation Creek 3 to Hells Hole 1. Individual measured sections are colorized and textured by facies (see figure 19), and lateral facies interpretation is colorized by facies association (grain size and carbonate textures, legend in figure 19). Predominant facies association trends are the laterally extensive carbonate shoals and littoral to sublittoral siltstones.*

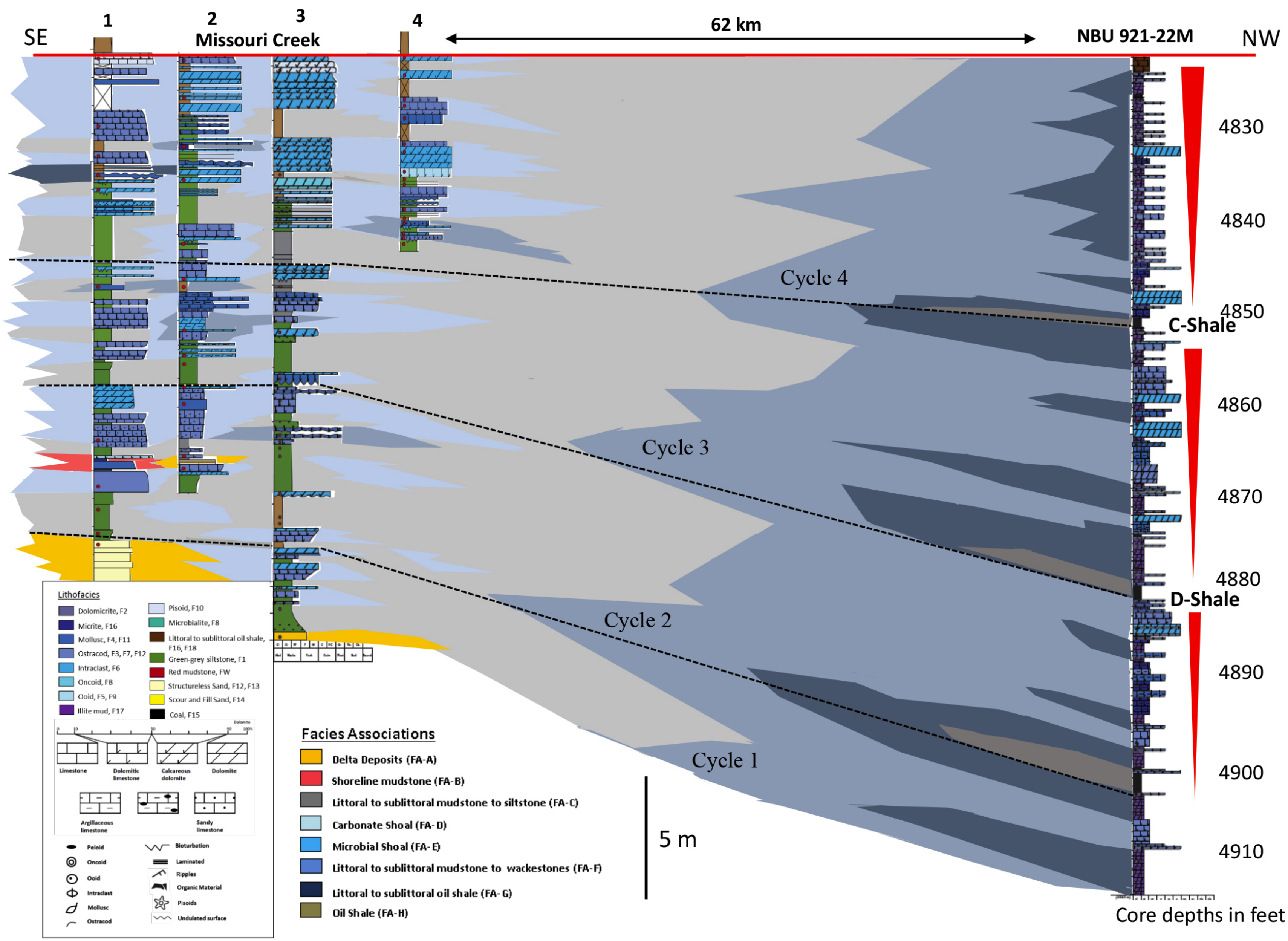

Figure 21. *Dip cross section from Missouri Creek Canyon to the NBU 921-22M core in the Greater Natural Buttes natural gas field. Major shallowing upward cycles are represented by red triangular cones next to core section. C- and D-shales are per Utah Geological Survey and oil company nomenclature. Individual measured sections are colorized and textured by facies (see figure 19) and lateral facies interpretation is colorized by facies association (grain size and carbonate textures as in legend on figure 19).*

Stratigraphic interpretations were based upon flooding surfaces marked by thin intraclastic rudstones and abrupt shift to deeper sublittoral mudrock. These correlations were made on the sub-regional scale between lake-margin environments as they changed laterally from calm backwater environments indicated by mud deposition to moderate energy, wave-influenced carbonate shoal settings, to fluvial environments that are preserved as sandy channel fill. Depositional cycles appear aggradational suggesting that sedimentation and accommodation were in balance. Correlation is possible from the lake margin into the deeper sublittoral basin where facies are highly laminated, organic rich, and thinly bedded. Facies showed major changes over the 62 km, but the four cycles are persistent into the deeper regions of the lake. Sublittoral successions are 30% thicker than the lake-margin Uteland Butte and are leaner in silt and richer in dolomite, nearly every bed contains >25% dolomite. The lakeward, and along depositional strike (Little, 1988), persistence of these cycles suggest an allocyclic control on deposition that can be tested as work on Uteland Butte is extended across the greater Lake Uinta area.

DIAGENESIS: CALCITE, DOLOMITE, AND POROSITY

Reservoir quality is an important issue in the Uteland Butte carbonates and this study included a preliminary examination of the early diagenesis that affected these carbonates. The following section summarizes the two most important early diagenetic changes to the Uteland Butte sediments, calcite cementation and dolomitization, which have had major impacts on the porosity in these rocks.

Calcite Cementation

Calcite is observed as cementation throughout the Uteland Butte in littoral facies and in some sublittoral facies. Two cement textures occur in the Uteland Butte samples, mosaic or granular cement and equant crystals. Cementation occurs between oolite, oncoid, and ostracod grains (figure 7C, figure 13A and B, figure 14B); in dissolved moldic pore spaces; as syntaxial overgrowths between peloids, ellipsoidal oncoids, and ostracod valves (figure 13E); and as equant mosaic calcite cementation in intraparticle pores (figure 13A). Cementation has significantly reduced porosity in packstones and grainstones. These cements are interpreted to represent early meteoric cementation in a lake environment undergoing lake level changes and fluvial input where carbonate-rich waters were present.

Dolomite

Dolomite/calcite ratios were determined through petrographic analysis and by QEMSCAN mineralogy scans. Varieties of Mg-rich carbonate range from stoichiometric dolomite to Mg-calcite, minerals that are very abundant in the Uteland Butte member (figure 22). The Uteland Butte carbonates typically contain between 25 to 50% dolomite with an average of 35%, most commonly as carbonate mud. The dolomudstone in the small QEMSCAN samples (1.5 cm X 1.5 cm areas) show a high percentage of dolomite (66–79%) and occur as intraclasts and peloids (figure 22). The intraclasts contain remnants of calcite. In both samples, calcite occurs as Mg-calcite and calcite. In figure 22B Mg-bearing calcite makes up 10.6% and calcite accounts for 9.7%. The same is the case for figure 22C where Mg-calcite is 23.5% and calcite is only 9.7%. Calcite occurs as bioclasts of bivalves and ostracods, and as calcite cement. In addition, dolomite is observed replacing ooid, oncoids, pisoids, and replacing the lime mud fill between ostracod shells. Dolomitic mud is rarely associated with mollusk and gastropod rudstones and floatstones.

Dolomite is also observed in core (figure 23). The F13 sublittoral oil shale is dolomite rich with laminations that host calcite ostracod shells and pyrite (figure 23A) and F7 intraclasts host green dolomite mud (figure 23B). Dolomitic bioclastic packstone to wackestones contain calcitic bivalve grains in a dolomitic mud matrix (figure 23C). F18 laminated dolomitic oil shales have possible burrows filled with calcite (pink), organic material (black), and silt size quartz (figure 23D).

The presence of dolomitic intraclasts in both the lake-margin and deeper lake area suggests early pre-burial replacement of lime mud in Mg-rich water with high organic content.

Porosity

FEI QEMSCAN 650F-Back Scatter Electron (BSE) system was the primary analysis tool used to evaluate microporosity within the facies of the Uteland Butte member. Initial estimates made from petrographic analysis underestimate porosity values, especially in fine-grained material where microporosity dominates. This is a result of the lower resolution of an optical microscope. The QEMSCAN-BSE detects and maps porosity and pore values as small as one micro-meter.

The QEMSCAN-BSE porosity analysis is run over several small areas (1.5 cm X 1.5 cm) to get a range and average porosity for each sample. Each scan produces three values, a porosity value, a porosity+mineral transition value, and a mineral amount. BSE relative intensity thresholds used to determine these values are: 0 to 27 porosity, 27 to 35 porosity+mineral transition, 35 + mineral. The porosity+mineral transition records porosity values detected between clear porosity and clearly defined mineral. In other studies (Jobe, 2013; Al-Suwaidi, 2015), other porosity measures such as CMS helium injection and mercury injection analyses indicate that this transition is dominantly porosity. Values discussed below are a sum of porosity and porosity/mineral transition values.

The Uteland Butte outcrop samples show varying amounts of micro- to nanoporosity. Porosity occurs in interparticle and in-

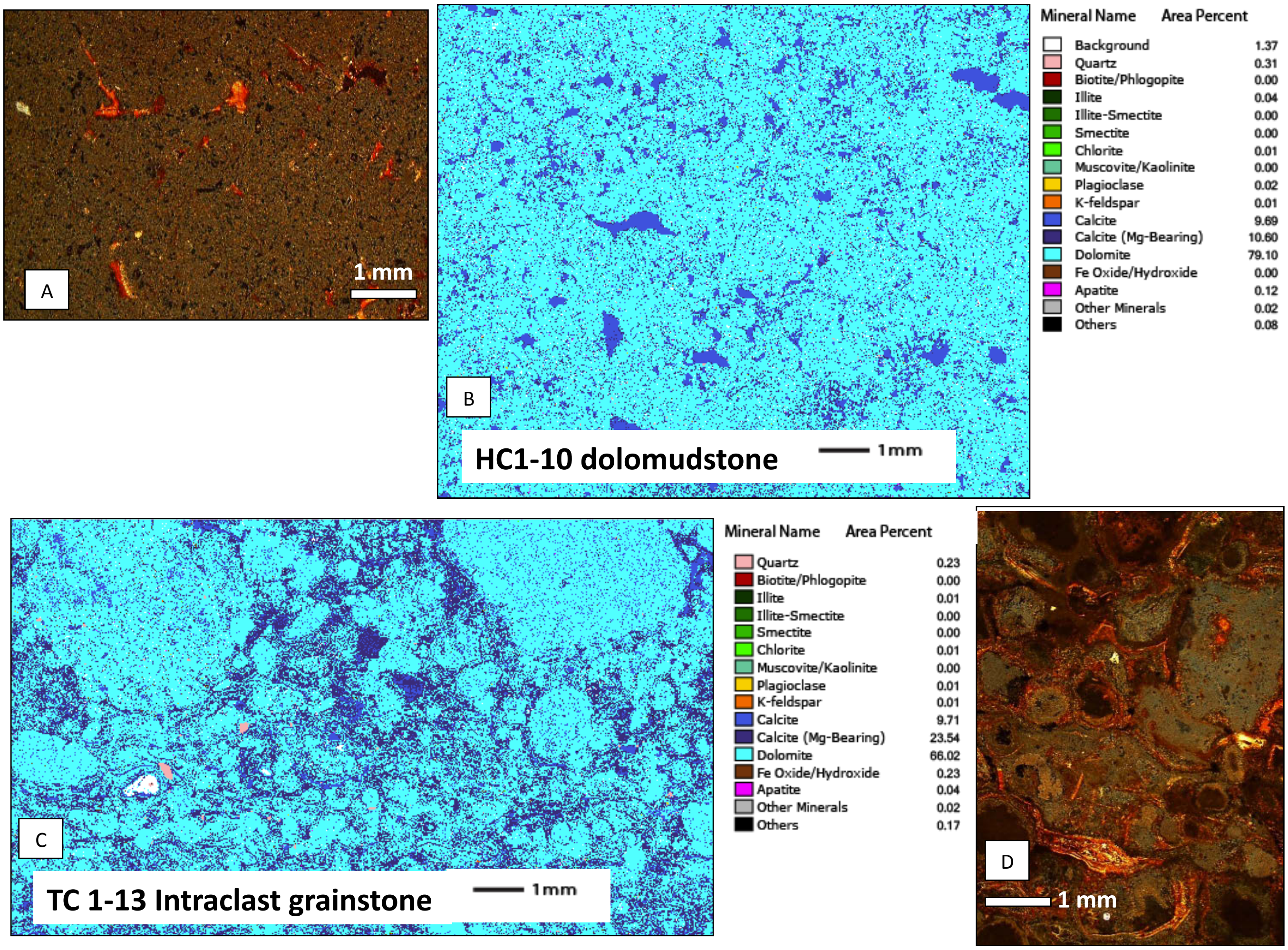

Figure 22. *Dolomite is most commonly observed in the Uteland Butte as a green to brown fine mud;* ***A.*** *Photomicrograph of (F2) lime to dolomite mudstone, organic rich with ostracod shells;* ***B.*** *QEMSCAN mineralogical scan of (A), dolomite composes 79.1% of the sample, and calcite ostracod shells and cement make up the remaining rock composition;* ***C.*** *Diagenesis did not completely alter calcite, intraclasts still contain some Mg-bearing calcite, though they are predominantly dolomitic. Clasts are coated in calcite cement (QEMSCAN mineral scan);* ***D.*** *Photomicrograph for (C), intraclast-peloid grainstone. Calcite fills interparticle pores and has occurred after dolomitization and rip-up of intraclast grains.*

traparticle pores and in dolomite mud as intercrystalline porosity. Dolomitic mud generally shows intercrystalline porosity, which ranges from 7 to 22%, and in size, from <1 to 5 micrometers (figure 24; F2, F7, and F9). Fracture and interparticle porosity is dominant in packstones, grainstones, rudstones, and floatstones, ranging from less than 1 to 8% (figure 24; F6, F8, and F10). Grainstones composed of peloid, ostracod, ooid, and oncoids also contain a wide variety of macroporosity types (figure 13B and D, figure 14B) from shelter to intraparticle in oncoids and some moldic porosity from bioclasts. Green siltstones (F1) have very low porosity (≤ 1%).

Although QEMSCAN-BSE scans were not run on core samples, the high concentration of fine-grained dolomite material supports a basic assumption that intercrystalline porosity may be common (figure 24; F2). Weatherford Labs measured porosity and permeability data using core plugs for several facies in the NBU-921-22m core. Porosity values and pore types are comparable to the outcrop estimates (table 3). Pore types are also consistent with the outcrop. The ostracod-intraclast packstone (F7) has primarily microporous intercrystalline porosity. The burrowed dolowackestone (F2) has intercrystalline microporosity with variable interconnectivity and a small amount of moldic pores and secondary pores. The argillaceous molluscan dolowackestone (F4) has intraparticle and intercrystalline porosity.

Despite the variety of facies analyzed, the pore size distribution observed was generally consistent across the eastern field area. Pore size distribution was calculated from digital pore extraction that calculates pore size with shape distribution. Isolated large macropores were avoided to keep from skewing QEMSCAN results. Pore size distribution for the eight facies displayed in figure 24 fell almost entirely into the range of 1 to 5 micro-meters. In dolomitic-mudrocks, <1 to 5 micro-meters represented about 90% of the pore size distribution. In calcareous mudstones, and coarser grained carbonate shoal facies, 5 to 10 micro-meters represented 15 to 25% of the pore size

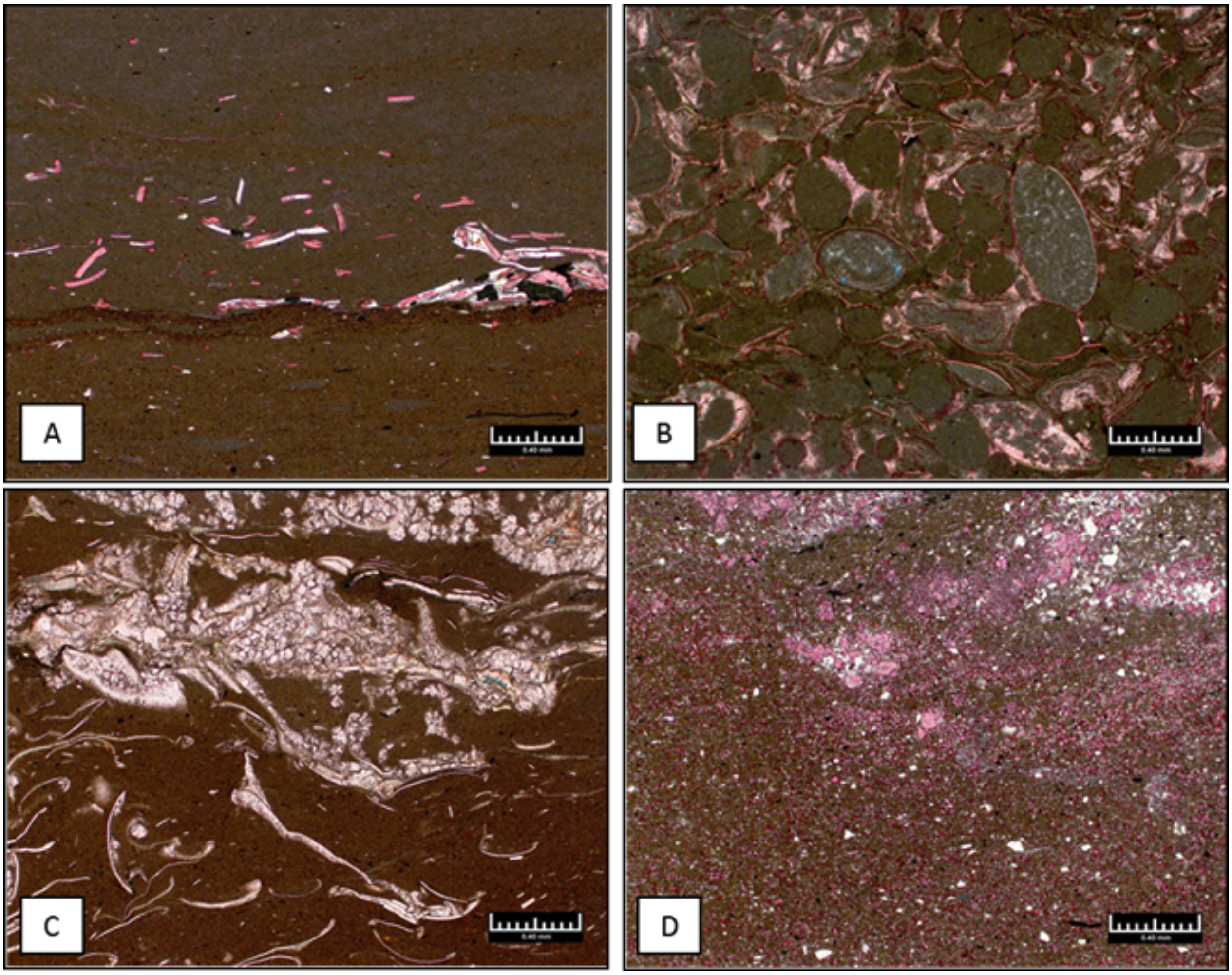

Figure 23. Dolomite diagenesis seen in core, all samples from NBU 921-22M, Anadarko Petroleum Company. ***A.*** *F3 ostracod lime mudstone-wackestone, argillaceous with black organic material, sample depth of 4868.65'*; ***B.*** *F7 ostracod lime packstone-grainstone, brown-green peloids are diagenetically replaced and commonly preserved within ostracod shells, calcite cement fills in between grains, sample depth of 4856.80 ft;* ***C.*** *F4 molluscan lime wackestone-packstone, mud is dolomitic while shell remains and grains around shells are calcite, sample depth of 4869.10 ft;* ***D.*** *Laminated oil shale with calcite replacement within interpreted burrowed sections, organic material and silt size quartz grains, sample depth of 4915 ft. Black scale bar is 0.40 mm.*

distribution, and <1 to 5 micro-meters represented the majority of the pore size distribution.

CONCLUSIONS

(1) The first major transgression of ancient Lake Uinta in the Uinta Basin was a highly cyclic, climatically driven, fresh, ostracod-rich, and molluscan-rich lake in which sediments underwent significant early dolomitization.

(2) The Uteland Butte lake-margin sediment is rich in silt and grainstone deposits, and the sublittoral deposits are thicker, highly laminated, finer grained, and contain more diagenetic dolomite. Dolomite mud is abundant, making up 25% to 50% of carbonate material, in marginal and sublittoral deposits.

(3) Four main cycles are preserved within the Uteland Butte member and are correlative from the lake margin into the deeper basin.

(4) Among the represented facies, porosity ranges between 1% and 20%, and permeability is usually below 1 md.

ACKNOWLEDGMENTS

This project was funded by the Utah Geological Survey via a grant from the U.S. Department of Energy, National Energy Technology Laboratory (DE-FE0010667). Funding was also provided by the Colorado School of Mines Green River Industrial Associates Consortium. The authors would like to thank the UGS reviewers who spent significant time editing this report and markedly improved the manuscript.

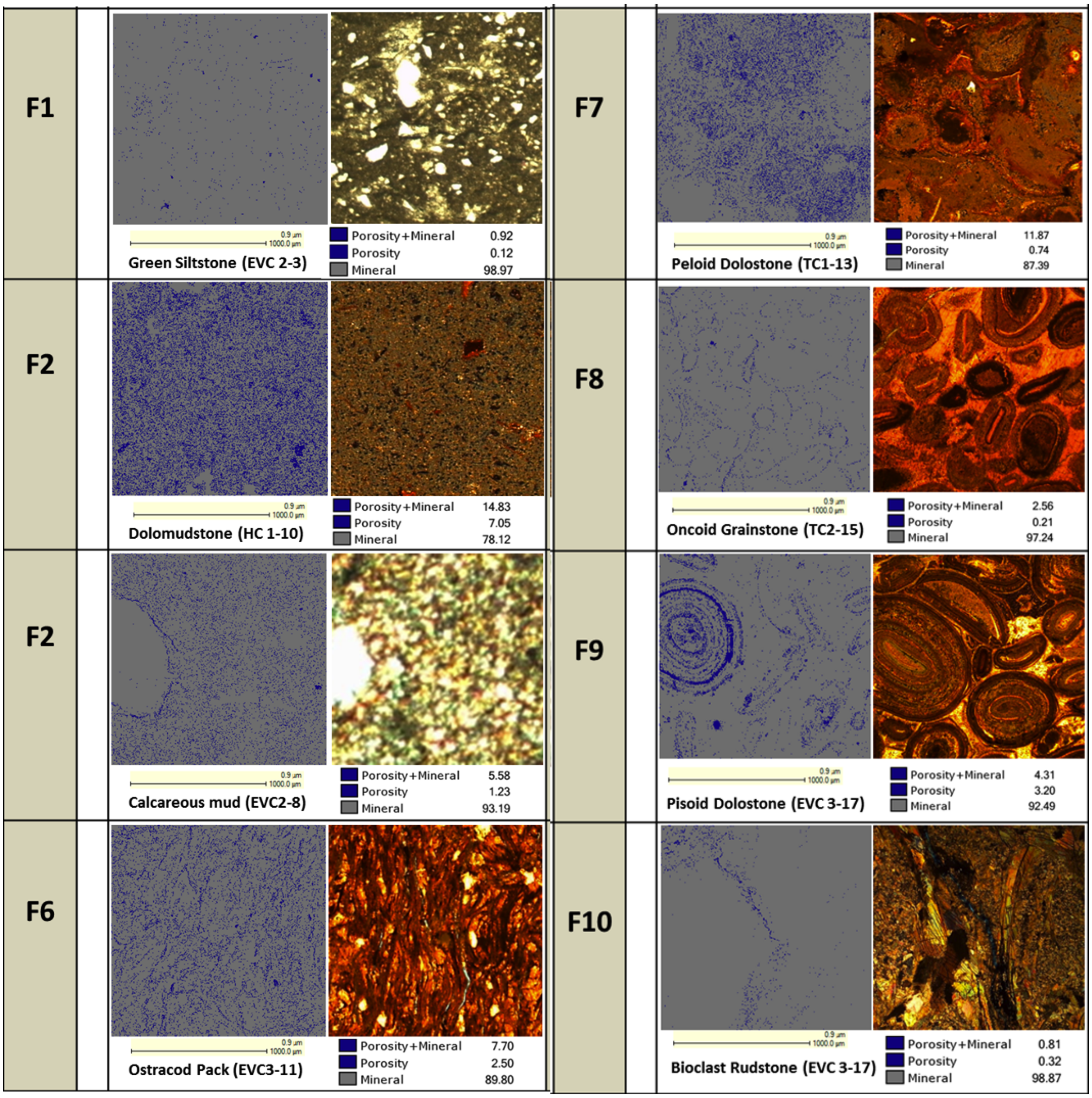

Figure 24. *Left is QEMSCAN images of F1, F2, and F6 displaying porosity >1 micro-meter and associated thin section photos. Right is QEMSCAN images of F7 through F10 displaying porosity >1 micro-meter and associated thin section photos. Porosity+mineral records an intensity transition from open pores to 100% mineral. Previous work shows that this transition is dominantly porosity.*

Table 3. *Porosity and permeability for Uteland Butte core samples (Weatherford analysis for Anadarko Petroleum).*

Lithofacies	Porosity (%)	Permeability (md)
Ostracod dolowackestone (F3)	12.2	1.23
Bioclastic dolowackestone (F4)	7.1	0.0053
Burrowed dolowackestone (F4)	2.8	0.092
Argillaceous molluscan dolowackestone (F4)	4.4	0.0001
Ostracod-intraclast packstone (F6)	6.9	0.0054
Dolograinstone (F6)	7.2	0.044
Bioclastic packstone (F11)	2.7	0.0001
Argillaceous dolomudstone (F17)	1.8	0.0011

REFERENCES

Abbott, W., 1957, Tertiary of the Uinta Basin: Utah Geological Association, Guidebook to the Geology of the Uinta Basin, eighth annual conference, 1957, p. 102–109.

Al-Suwaidi, M.E., 2015, Lower Bab Member (A0)— A study of sequence stratigraphy, porosity characterization, and tight reservoir development, Abu Dhabi, UAE: Golden, Colorado School of Mines, Ph.D. dissertation, 147 p.

Birdwell, J.E., Vanden Berg, M.D., Johnson, R.C., Mercier, T.J., Boehlke, A.R., and Brownfield, M.E., in press, Geological, geochemical, and reservoir characterization of the Uteland Butte member of the Green River Formation, Uinta Basin, Utah: Rocky Mountain Association of Geologists, Source Rock Compendium.

Bohacs, K.M., Carroll, A.R., Neal, J.E., and Mankiewicz, P.J., 2000, Lake-basin type, source potential, and hydrocarbon character—an integrated sequence-stratigraphic-geochemical framework, *in* Gierlowski-Kordesch, E.H., and Kelts, K.R., editors, Lake Basins through space and time: American Association of Petroleum Geologists Bulletin, v. 83, p. 3–34.

Bradley, W.H., 1931, Origin and microfossils of the oil shale of the Green River Formation of Colorado and Utah: U.S. Geological Survey Professional Paper 168, p. 58.

Burton, D., Woolf, K., and Sullivan, R., 2014, Lacustrine depositional environments in the Green River Formation, Uinta Basin—Expression in outcrop and wireline logs: American Association of Petroleum Geologists Bulletin, v. 98, no. 9, p. 1699–1715.

Bustillo, M.A., Arribas, M.E., and Bustillo, M., 2002, Dolomitization and silicification in low-energy lacustrine carbonates (Paleogene, Madrid Basin, Spain): Sedimentary Geology, v. 151, p. 107–126.

Carroll, A.R., Chetel, L.M., and Smith, M.E., 2006, Feast to famine—Sediment supply control on Laramide basin fill: Geology, v. 34, p. 197–200.

Cashion, W.B., and Donnell, J.R., 1972, Chart showing the correlation of selected key units in the organic-rich sequence of the Green River Formation, Piceance Creek basin, Colorado and Uinta basin, Utah: U.S. Geological Survey Bulletin B-1394-G, 9p.

Cashion, W.B., and Donnell, J.R., 1974, Revision of nomenclature of the upper part of the Green River Formation, Piceance Creek Basin, Colorado, and eastern Uinta Basin, Utah: U.S. Geological Survey Bulletin B-1396-G, 9p.

Cohen, A.S., 2003, Paleolimnology: Oxford University Press, Oxford, p. 500.

Cole, R.D., and Picard, M.D., 1978, Comparative mineralogy of nearshore and offshore lacustrine lithofacies, Parachute Creek Member of the Green River Formation, Piceance Creek Basin, Colorado, and eastern Uinta Basin, Utah: Geological Society of America Bulletin, v. 89, p. 1441–1454.

Davis, S.J., Wiegard, B.A., Carroll, A.R., and Chamberlain, C.P., 2008, The effect of drainage reorganization on paleoaltimetry studies—an example from the Paleogene Laramide foreland: Earth and Planetary Science Letters 275, p. 258–268.

Davis, S.J., Mulch, A., Carroll, A.R., Horton. T.W., and Chamberlain, C.P., 2009, Paleogene landscape evolution of the central North America Cordillera—developing topography and hydrology in the Laramide foreland: Geological Society of America Bulletin, v. 120, p. 100–133.

Davis, S.J., Mix, H.T., Weigand, B.A. Carroll, A.R., and Chamberlain, C.P, 2010, Synorogenic evolution of large-scale drainage patterns—isotope paleohydrology of sequential Laramide basins: American Journal of Science, v. 309, p. 549–602.

Dickinson, W.R., Klute, M.A., Hayes, M.J., Janecke, S.U., Lundin, E.R., McKittrick, M.A., and Olivares, M.D., 1988, Paleogeographic and paleotectonic setting of Laramide sedimentary basins in the central Rocky Mountain region: Geological Society of America Bulletin, v. 100, p. 1023–1039.

Dunham, R.J., 1962, Classification of carbonate rocks according to depositional textures: American Association of Petroleum Geologists Memoir 1, p. 108–121.

Dyni, J.R., and Hawkins, J.E., 1981, Lacustrine turbidites in the Green River Formation, northwestern Colorado: Geological Society of America Bulletin, v. 9, no. 5, p. 235–238.

Dyni, J.R., 2006, Geology and resources of some world oil-shale deposits: U.S. Geological Survey Scientific Invest. Rep. 2005-5294, 42 p.

Embry, A.F., and Klovan, J.E., 1971, A Late Devonian reef tract on northeastern Banks Island, N.W.T.: Bulletin of Canadian Petroleum Geology, v. 19, p. 730–761.

Eugster, H.P., and Hardie, L.A., 1978, Saline lakes, *in* Lermand, A., editor, Lakes—Chemistry, geology, physics: Springer, Berlin, p. 238–293.

Fouch, T.D., Nuccio, V.F., Osmond, J.C., MacMillan, L., Cashion, W.B., and Wandrey, C.J., 1992, Oil and gas in uppermost Cretaceous and Tertiary rock, Uinta Basin, Utah, *in* Fouch, T.D., Nuccio, V.F., and Chidsey, T.C., editors, Hydrocarbon and mineral resources of the Uinta Basin, Utah and Colorado: Utah Geological Association, Guidebook 20, p. 9–47.

Franczyk, K.J., Fouch, T.D., Johnson, R.C., Molenaar, C.M., and Cobban, W.A., 1992, Cretaceous and Tertiary paleogeographic reconstructions for the Uinta-Piceance Basin study area, Colorado and Utah: U.S. Geological Survey Bulletin B-1787-Q, p. 1–37.

Gierlowski-Kordesch, E.H., 2010, Lacustrine carbonates, *in* Alonso-Zarza, A.M., and Tanner, L.H., editors, Carbonates in continental settings—Facies, environments, and processes: Elsevier, Developments in Sedimentology 61, p. 1–101.

Hasiotis, S.T., and Honey, J.G., 2000, Paleohydrologic and stratigraphic significance of crayfish burrows in continental deposits—examples from several Paleocene Laramide basins in the Rocky Mountains: Journal of Sedimentary Research, 70, p. 127–139.

Jobe, T.D., 2013, Sedimentology, chemostratigraphy and quantitative pore architecture in microporous carbonates—examples from a giant oil field offshore Abu Dhabi, UAE: Golden, Colorado School of Mines, Ph.D. dissertation, 143 p.

Johnson, T.C., 1984, Sedimentation in large lakes: Annual Review of Earth and Planetary Sciences 12, p. 179–204.

Johnson, R.C., 1985a, New names for units in the lower part of the Green River Formation, Piceance Creek Basin, Colorado: U.S. Geological Survey Bulletin 1529-I, p. 20.

Johnson, R.C., 1985b, Early Cenozoic history of the Uinta and Piceance Creek Basins, Utah and Colorado, with special reference to the development of Eocene Lake Uinta, *in* Flores, R.M., and Kaplan, S.S., editors, Cenozoic paleogeography of the west-central United States: Rocky Mountain Section, Society of Economic Paleontologists and Mineralogists, Denver, CO., p. 247–276.

Johnson, R.C., Mercier, T.J., Michael, B.E., and Self, J.G., 2010, Assessment of in-place oil shale resources in the Eocene Green River Formation, Uinta Basin, Utah and Colorado: U.S. Geological Survey, Chapter 1, p. 4–162.

Keighley, D., Flint, S., Howell, J., and Moscariello, A., 2003, Sequence Stratigraphy in Lacustrine Basins—A model for part of the Green River Formation (Eocene), southwest Uinta Basin, Utah, U.S.A.: Journal of Sedimentary Research, v. 73, no. 6, p. 987–1006.

Little, T.M., 1988, Depositional environments, petrology, and diagenesis of the basal limestone facies, Green River Formation (Eocene), Uinta basin, Utah: Salt Lake City, University of Utah, M.S. thesis, 154 p.

Morgan, C.D., and Bereskin, S.R., 2003, Characterization of petroleum reservoirs in the Eocene Green River Formation, central Uinta Basin, Utah: The Mountain Geologist, v. 39, no. 4, p. 111–127.

Morgan, C.D., Chidsey, T.C., Jr., McClure, K.P., Bereskin, S.R., and Deo, M.D., 2003, Reservoir characterization of the lower Green River Formation, Uinta Basin, Utah: Utah Geological Survey Open-File Report, 411, 140 p.

Osmond, J.C., 1965, Geologic history of site of Uinta Basin, Utah: American Association of Petroleum Geologists Bulletin, v. 49, no. 11, p. 1957–1973.

Picard, M. D., 1957, Green River and Lower Uinta Formations—Subsurface stratigraphic changes in central and eastern Uinta Basin, Utah: Utah Geological Association Guidebook, p. 116–130.

Pietras, J.T., Carroll, A.R., Singer, B.S., and Smith, M.E., 2003, 10 k.y. depositional cyclicity in the early Eocene—Stratigraphic and $^{40}Ar/^{39}Ar$ evidence from the lacustrine Green River Formation: Geological Society of America, v. 31, no. 7, p. 593–596.

Pitman, J.K., 1996, Origin of primary and diagenetic carbonates in the lacustrine Green River Formation (Eocene), Colorado and Utah: U.S. Geological Survey Bulletin 2157, p. 1–16.

Platt, N.H., and Wright, V.P., 1991, Lacustrine carbonates—facies models, facies distributions and hydrocarbon aspects, *in* Anadon, P., Cabrera, L., Kelts, K., editors, Lacustrine facies analysis: International Association of Sedimentologists Special Publication, v. 13, p. 57–74.

Reading, H.G., and Collinson, J.D., 1996, Clastic coasts, *in* Reading, H.G., editor, Sedimentary Environments: Processes, Facies and Stratigraphy, 3rd edition, Blackwell Science, Oxford, p. 154–231.

Remy, R.R., 1992, Stratigraphy of the Eocene part of the Green River Formation in the south-central part of the Uinta Basin, Utah: U.S. Geological Survey Bulletin B-1787-BB, p. 1–69.

Renaut, R.W., and Gierlowski-Kordesch, E.H., 2010, Lakes, *in* James, N.P., and Dalrymple, R.W., editors, Facies Models: Geological Association of Canada, IV Series, GEOtext 6, p. 541–575.

Rosenberg, M.J., Birgenheier, L.P., and Vanden Berg, M.D., 2015, Facies, stratigraphic architecture, and lake evolution of the oil shale bearing Green River Formation, eastern Uinta Basin, Utah, *in* Smith, M.E., and Carroll, A.R., editors, Stratigraphy and paleolimnology of the Green River Formation, western USA: Springer, DOI 10.1007/978-94-017-9906-5, p. 211–249.

Ryder, R.T., Fouch, T.D., and Elison, J.H., 1976, Early Tertiary sedimentation in the western Uinta Basin, Utah: Geological Survey of America Bulletin, v. 87, p. 496–512.

Schamel, S., 2015, Rediscovered shale oil resource play potential of the Green River Formation, Uinta Basin, Utah—Associated with energy resource development, *in* Vanden Berg, M.D., Ressetar, R., and Birgenheier, L.P., editors, Geology of Utah's Uinta Basin and Uinta Mountains: Utah Geological Association Publication 44, p. 275–303.

Schomacker, E.R., Kjemperud, A.V., Nystuen, J.P., and Jahren, J.S., 2010, Recognition and significance of sharp-based mouth-bar deposits in the Eocene Green River Formation, Uinta basin, Utah: Sedimentology, v. 57, p. 1069–1087.

Self, J.G., Brownfield, M.E., Johnson, R.C., and Mercier, T.J., 2010a, Fischer assay histograms of oil shale drill cores and cuttings from the Uinta basin, Utah and Colorado:

U.S. Geological Survey, Digital Data Series DDS–69–BB, chapter 5, 8 p.

Self, J.G., Brownfield, M.E., Johnson, R.C., and Mercier, T.J., 2010b, Fischer assay histograms of oil shale drill cores and cuttings from the Piceance Basin, northwestern Colorado: U.S. Geological Survey, Digital Data Series DDS–69–Y, chapter 7, 9 p.

Smith, M.E., Carroll, A.R., and Singer, B.S., 2008, Synoptic reconstruction of a major ancient lake system—Eocene Green River Formation, western United States: Geological Society of America Bulletin, v. 120, n. 1, p. 1–54.

Smith, M.E., Chamberlain, K.R., Singer, B.S., and Carroll, A.R., 2010, Eocene clocks agree—coeval $^{40}Ar/^{39}Ar$, U-Pb, and astronomical ages from the Green River Formation: Geology, v. 38, p. 527–530.

Smoot, J.P., 1983, Depositional subenvironments in an arid closed basin—the Wilkins Peak Member of the Green River Formation, western United States: Geological Society of America Bulletin, v. 120, p. 54–84.

Strohmenger, C., and Wirsing, G., 1991, A proposed extension of Folk's (1959, 1962) textural classification of carbonate rocks: Carbonate and Evaporites, Springer Link, v. 6, p. 23–28.

Tänavsuu-Milkeviciene, K., and Sarg, J.F., 2012, Evolution of an organic-rich lake basin—stratigraphy, climate and tectonics—Piceance Creek Basin, Eocene Green River Formation: Sedimentology, v. 59, p. 1735–1768.

Taylor, A.W., and Ritts, B.D., 2004, Mesoscale heterogeneity of fluvial lacustrine reservoir analogues—examples from the Eocene Green River Formation and Colton Formations, Uinta Basin, Utah, USA: Journal of Petroleum Geology, v. 27, p. 3–25.

Tucker, M.E., and Wright, V.P., 1990, Carbonate sedimentology: Blackwell Scientific Publications, Oxford, 482 p.

Vanden Berg, M.D., 2008, Basin-wide evaluation of the uppermost Green River Formation's oil-shale resource, Uinta basin, Utah and Colorado: Utah Geological Survey Special Study 128, p. 1–23.

Vanden Berg, M.D., Wood, R.E., Carney, S.M., and Morgan, C.D., 2014, Geological characterization of the Uteland Butte Member of the Eocene Green River Formation—an emerging unconventional carbonate tight oil play in the Uinta Basin, Utah: 2014 Rocky Mountain Section of the American Association of Petroleum Geologists Annual Meeting, July 20–22, 2014, Program with Abstracts, p. 44.

Wiggins, W.D., and Harris, P.M., 1994, Lithofacies, depositional cycles, and stratigraphy of the lower Green River Formation, southwestern Uinta Basin, Utah: Society for Sedimentary Geology, Core Workshop No. 19, p. 105–141.